E-Glider: Active Electrostatic Flight Concept for Airless Body Exploration

Dr. Marco B. Quadrelli
Jet Propulsion Laboratory/Caltech

Reference herein to any specific commercial product, process, or service by trade name, trademark, manufacturer, or otherwise, does not constitute or imply its endorsement by the United States Government or the Jet Propulsion Laboratory, California Institute of Technology.

Pre-Decisional Information -- For Planning and Discussion Purposes Only
© 2016 California Institute of Technology. Government sponsorship acknowledged.

marco.b.quadrelli@jpl.nasa.gov

Solar driven circumnavigation
(insert from Aplin, 2008)

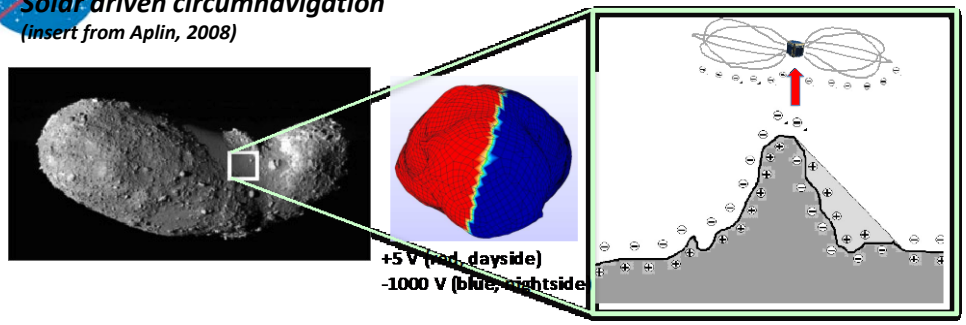

E-Glider concepts

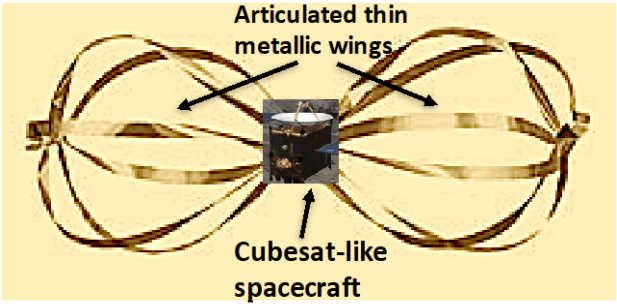

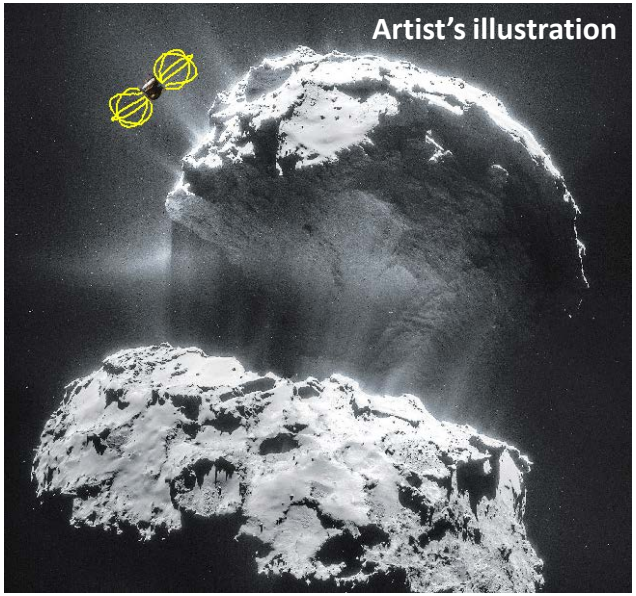

www.rosetta.esa.int

E-Glider: A Concept for Active Electrostatic Flight Concept for Airless Body Exploration

Dr. Marco B. Quadrelli (P.I., JPL)
Co-I's: Henry Garrett, Masahiro Ono, Adrian Stoica, Julie Castillo (JPL)
Christine Hartzell (Univ. of Maryland)
Hanspeter Schaub (Univ. of Colorado Boulder)
marco.b.quadrelli@jpl.nasa.gov

Navigation based on electrostatic cartography

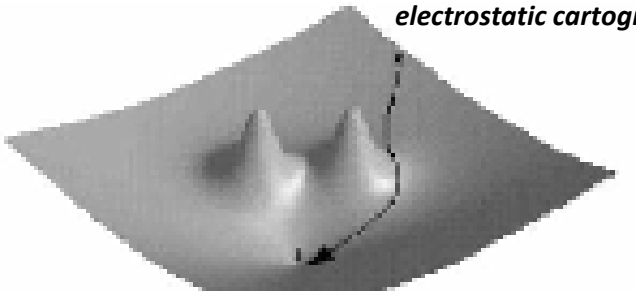

Electrostatic inflation tests *(Stiles & Schaub, 2010)*

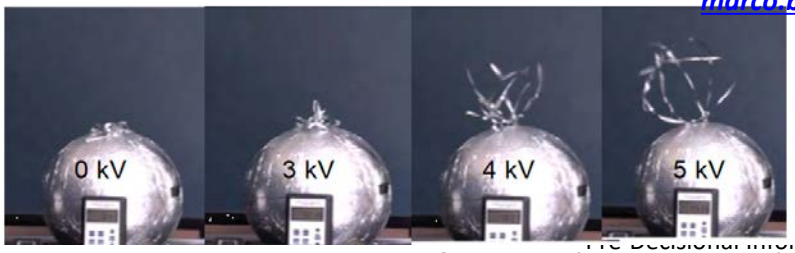

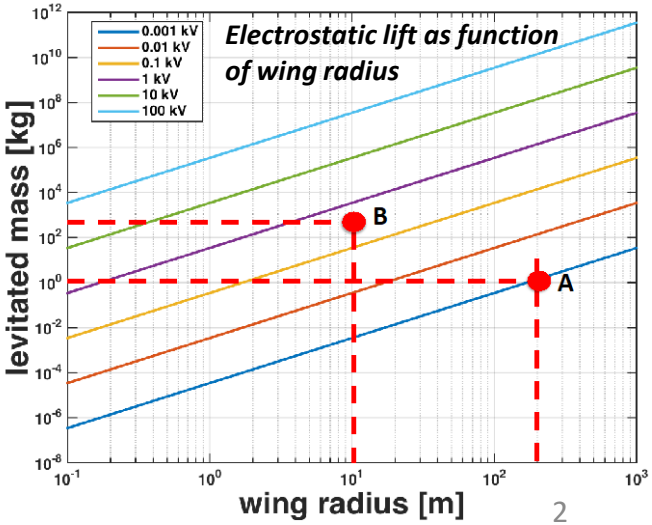

Pre-Decisional Information -- For Planning and Discussion Purposes Only
© 2016 California Institute of Technology. Government sponsorship acknowledged.

Team

- Dr. Marco Quadrelli, P.I., flight dynamics expert
- Dr. Henry Garrett, JPL space charging expert
- Dr. Julie Castillo, Asteroid Scientist
- Dr. Adrian Stoica, Robotics Autonomy expert
- Dr. Hiro Ono, Robotics Path Planning expert
- Prof. Christine Hartzell, UMD, asteroid electrostatic dust expert
- Prof. Hanspeter Schaub, U. Colorado Boulder, expert on electrostatic inflation systems

Students (mentored by Marco):

- Caleb Christianson (UCSD), Dario Lusso, Simone Fasiello, (Polytechnic of Turin, Italy), Shota Kikuchi (Univ. of Tokyo/Purdue University)

Pre-Decisional Information -- For Planning and Discussion Purposes Only
© 2016 California Institute of Technology. Government sponsorship acknowledged.

marco.b.quadrelli@jpl.nasa.gov

What is an E-Glider?

- The environment near the surface of airless bodies (asteroids, comets, moons) is electrically charged due to Sun's photoelectric bombardment.

- Charged dust is ever present, even at high altitudes (dust fountains), following the Sun's illumination.

- We envisage the global scale exploration of airless bodies by a gliding vehicle that levitates by experiencing electrostatic lift by its interaction with the naturally charged particle environment.

- This Electrostatic Glider (E-Glider) lifts off by extending thin, charged, appendages (like some flying spiders on Earth), which are also articulated to direct the levitation force in the most convenient direction for propulsion and maneuvering. It lands, wherever it is most convenient, by retracting the appendages or by thruster/anchor.

Pre-Decisional Information -- For Planning and Discussion Purposes Only
© 2016 California Institute of Technology. Government sponsorship acknowledged.

marco.b.quadrelli@jpl.nasa.gov

The E-Glider in operation

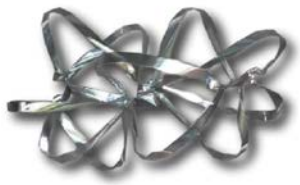

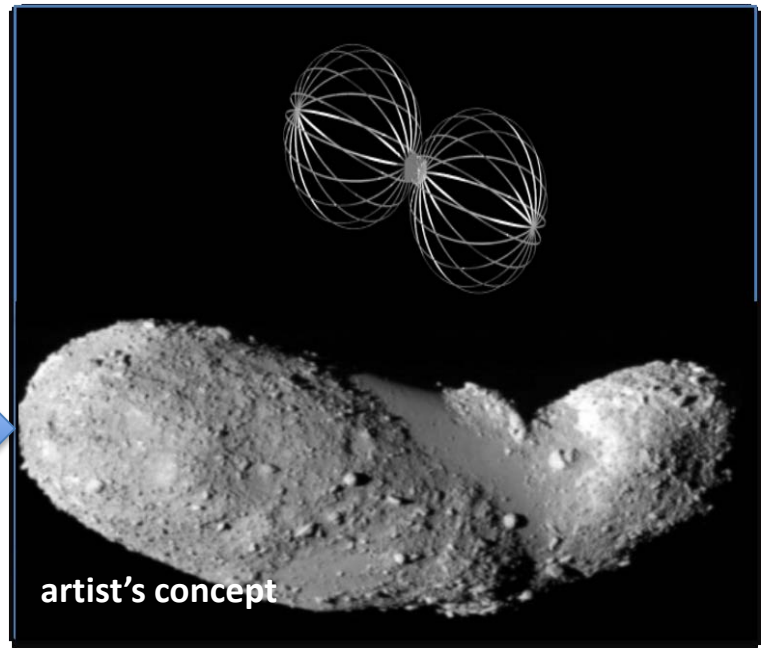

Courtesy Unitech Toys, Co.

Pre-Decisional Information -- For Planning and Discussion Purposes Only
© 2016 California Institute of Technology. Government sponsorship acknowledged.

marco.b.quadrelli@jpl.nasa.gov

Benefits

- The E-Glider concept directly addresses the "All Access Mobility" Challenge, one of the NASA's Space Technology Grand Challenges, specifically aimed at enabling robotic operations and mobility, in the most extreme environments of our solar system.
- We'll be able to circumnavigate/map, reconnoiter airless bodies at low cost
- We'll be able to do unconventional in-situ science without necessarily landing on surface
- We'll have invented a new area of spacecraft technology: electrostatic flight technology
- We may be able to lead to new forms of transportation on the Earth.

Pre-Decisional Information -- For Planning and Discussion Purposes Only
© 2016 California Institute of Technology. Government sponsorship acknowledged.
marco.b.quadrelli@jpl.nasa.gov

Science Value

- The E-glider would be able to support diverse science needs at diverse sites, since the lander is now much more agile on account of its maneuverability and lofting capability all around the body of interest, such as in-situ plasma measurements at different spatial and temporal scales, and distributed gravity field measurements.

- Exploration of comets, asteroids, moons and planetary bodies is limited by mobility on those bodies. Current robotic and human systems cannot safely traverse a number of prevalent surface terrains, and travel slowly, requiring detailed oversight and planning activities. Consequently, these systems are often limited to exploring areas close to their original landing site. The lack of an atmosphere, the low gravity levels, and the unknown surface soil properties pose a very difficult challenge for all forms of know locomotion.

Pre-Decisional Information -- For Planning and Discussion Purposes Only
© 2016 California Institute of Technology. Government sponsorship acknowledged.
marco.b.quadrelli@jpl.nasa.gov

What Phase I proposes to do

We'll have identified an approach to:

- Navigate to do useful science with E-glider
- successful charge balance and maintenance of the vehicle,
- the approach to differentially charge the surfaces so that electro-maneuvering can be achieved.

Phase II:

- Small scale ground tests in vacuum chamber
- Particle-in-cell simulation of vehicle flying immersed in dusty plasma around asteroid
- Ultimately, flight demo with cubesat on Moon surface

Pre-Decisional Information -- For Planning and Discussion Purposes Only
© 2016 California Institute of Technology. Government sponsorship acknowledged.

marco.b.quadrelli@jpl.nasa.gov

Phase I approach

- Analyze a mission scenario involving an electrostatic glider maneuvering above the surface of a reference asteroid, such as Itokawa:

- Study the known environmental conditions of the electrostatics of the lofting dust on the surface of airless bodies;

- Determine E-glider vehicle configurations, and specific methods for energy harvesting, mobility, communication, survivability, and instruments for in-situ sampling of dust and surface regolith; and

- Explore the possibility of generating (in Phase II) physical simulations and small-scale experiments with approximate models of the E-glider, including their energy harvesting, mobility, and comm. mechanisms.

Pre-Decisional Information -- For Planning and Discussion Purposes Only
© 2016 California Institute of Technology. Government sponsorship acknowledged.
marco.b.quadrelli@jpl.nasa.gov

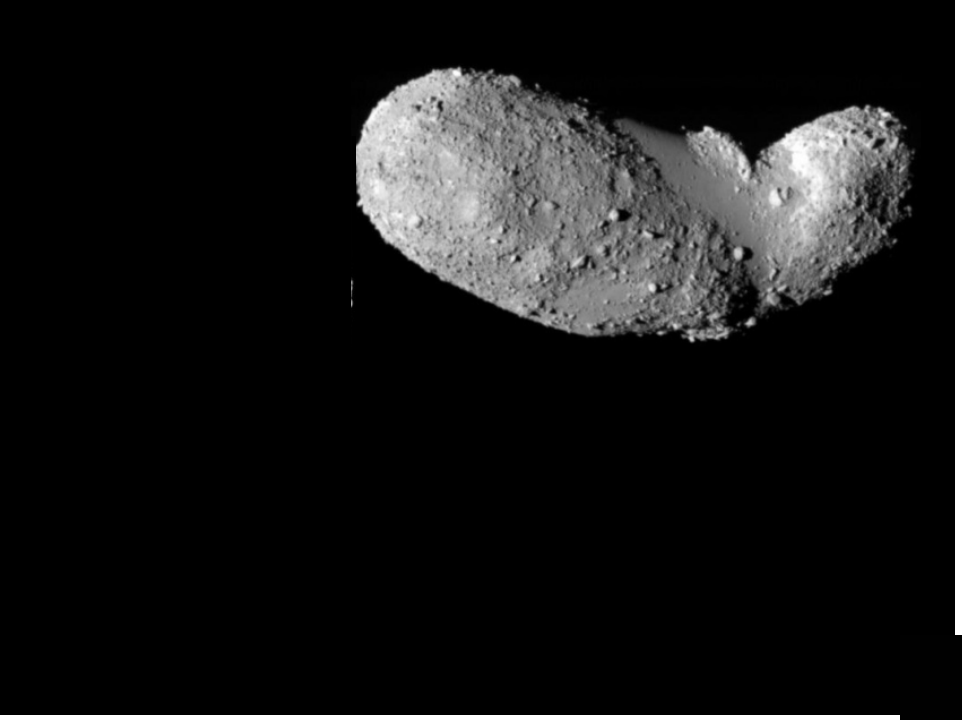

Challenges of small bodies

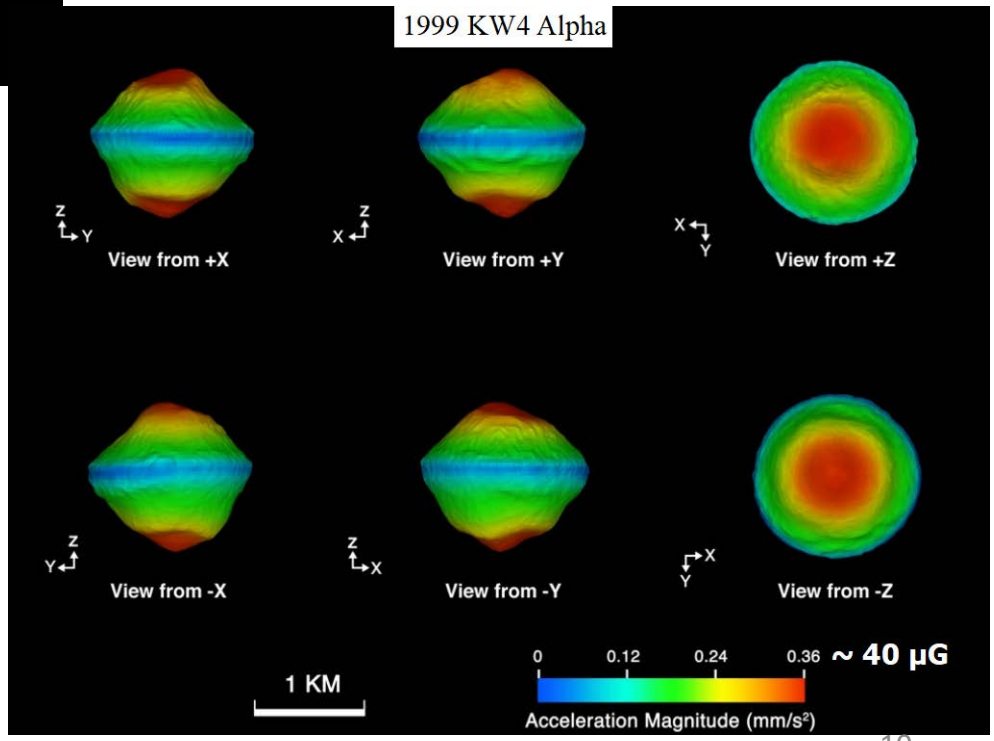

Physics at airless bodies

- **Cohesion Forces:** Can dominate particle interactions through van der Waals forces.
- **Solar radiation:** Not relevant unless a particle is lofted and cohesive force removed
- **Electrostatics:** Negligible except at terminator where it can lead to significant dust transport

Pre-Decisional Information -- For Planning and Discussion Purposes Only
© 2016 California Institute of Technology. Government sponsorship acknowledged.

marco.b.quadrelli@jpl.nasa.gov

Small body gravity

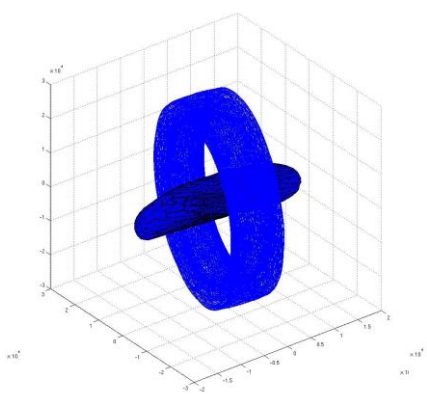

Stable Orbits around 433 Eros

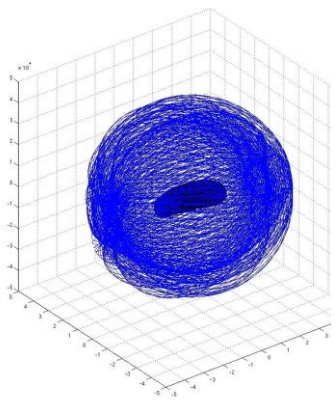

Unstable Orbits around 433 Eros

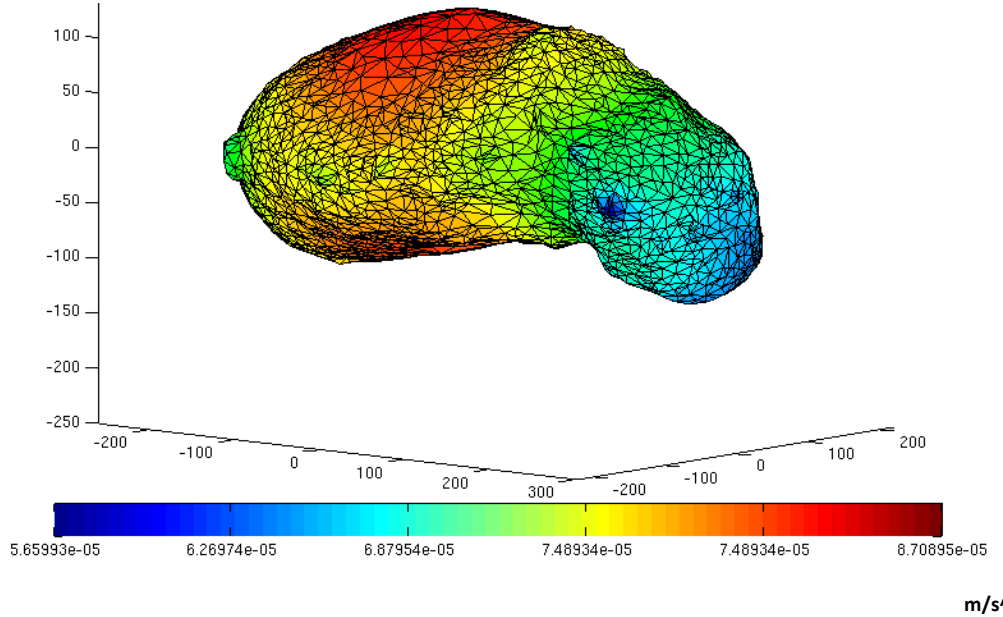

Itokawa Total Surface Acceleration

Gravity Order of Magnitude	Total Surface Acceleration	Body
1 G	1 G	Earth
0.1 G	0.17 G	Moon
1 milli-G	0.2 to 0.6 milli-G	Eros (18 km)
10 micro-G	6-9 micro-G	Itokawa (0.18 km)

Pre-Decisional Information -- For Planning and Discussion Purposes Only
© 2016 California Institute of Technology. Government sponsorship acknowledged.

marco.b.quadrelli@jpl.nasa.gov

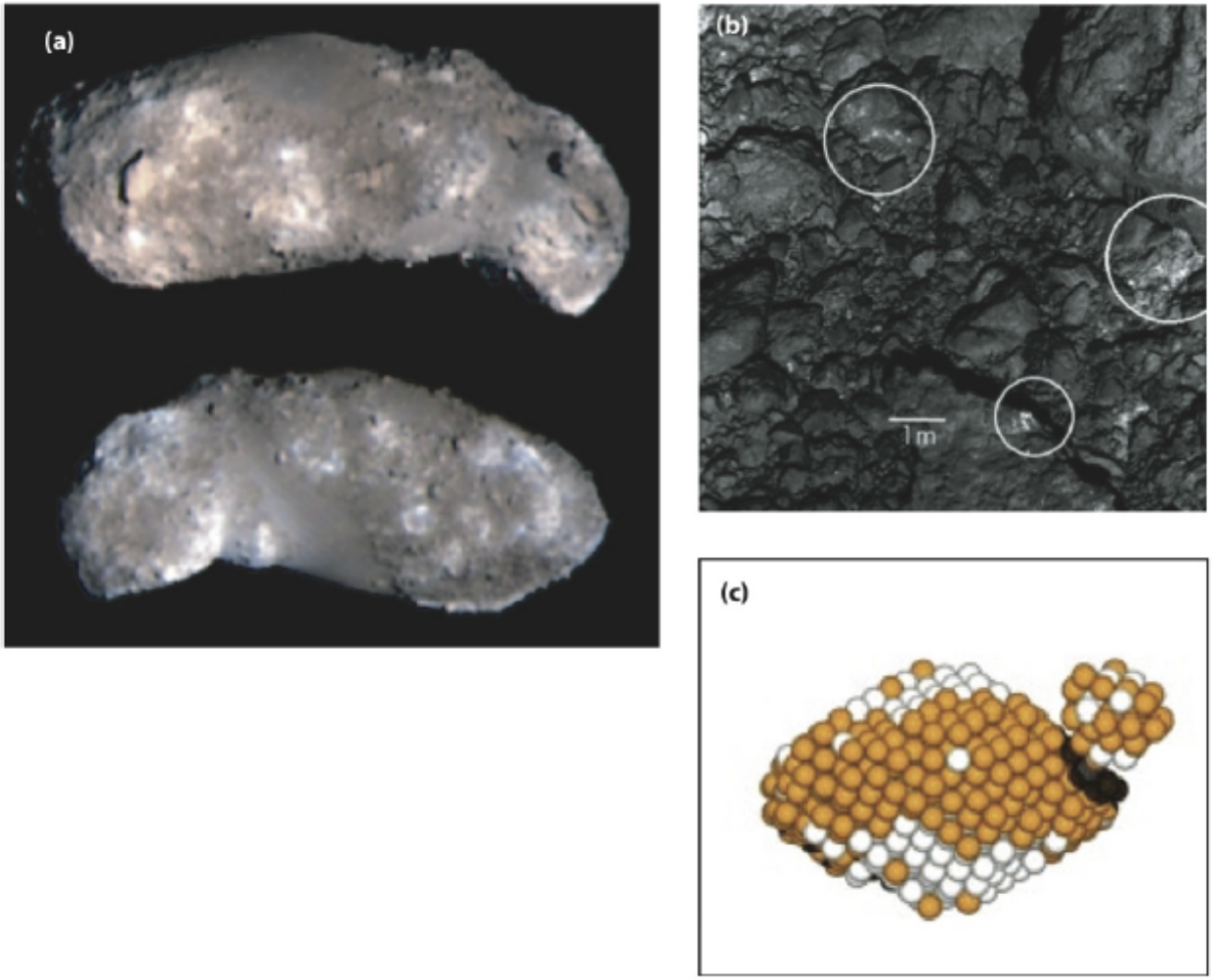

Figure 5. (a) Chemical and physical property variations observed at the surface of Itokawa by the *Hayabusa* mission. The surface shows significant lateral variations in roughness determined in large part the gravity field. Local surface overturn (due to landslides or impacts) has exposed fresh material whose high albedo significantly contrasts with the overall dark color of the asteroids weathered surface. (b) High-resolution view of the surface illustrating the hazardous conditions presented by that type of bodies to Human exploration. (c) Result of the simulation of binary asteroid formation [39] as a consequence of high-velocity spinning of the original parent body; spinning results in the redistribution of material from the equator to the poles and the exposure of pristine material (orange) buried below the regolith layer (white).

Courtesy of Julie Castillo-Rogez, JPL

Pre-Decisional Information -- For Planning and Discussion Purposes Only
© 2016 California Institute of Technology. Government sponsorship acknowledged.

marco.b.quadrelli@jpl.nasa.gov

Rotation Period vs. Diameter, 2010, 3643 Asteroids

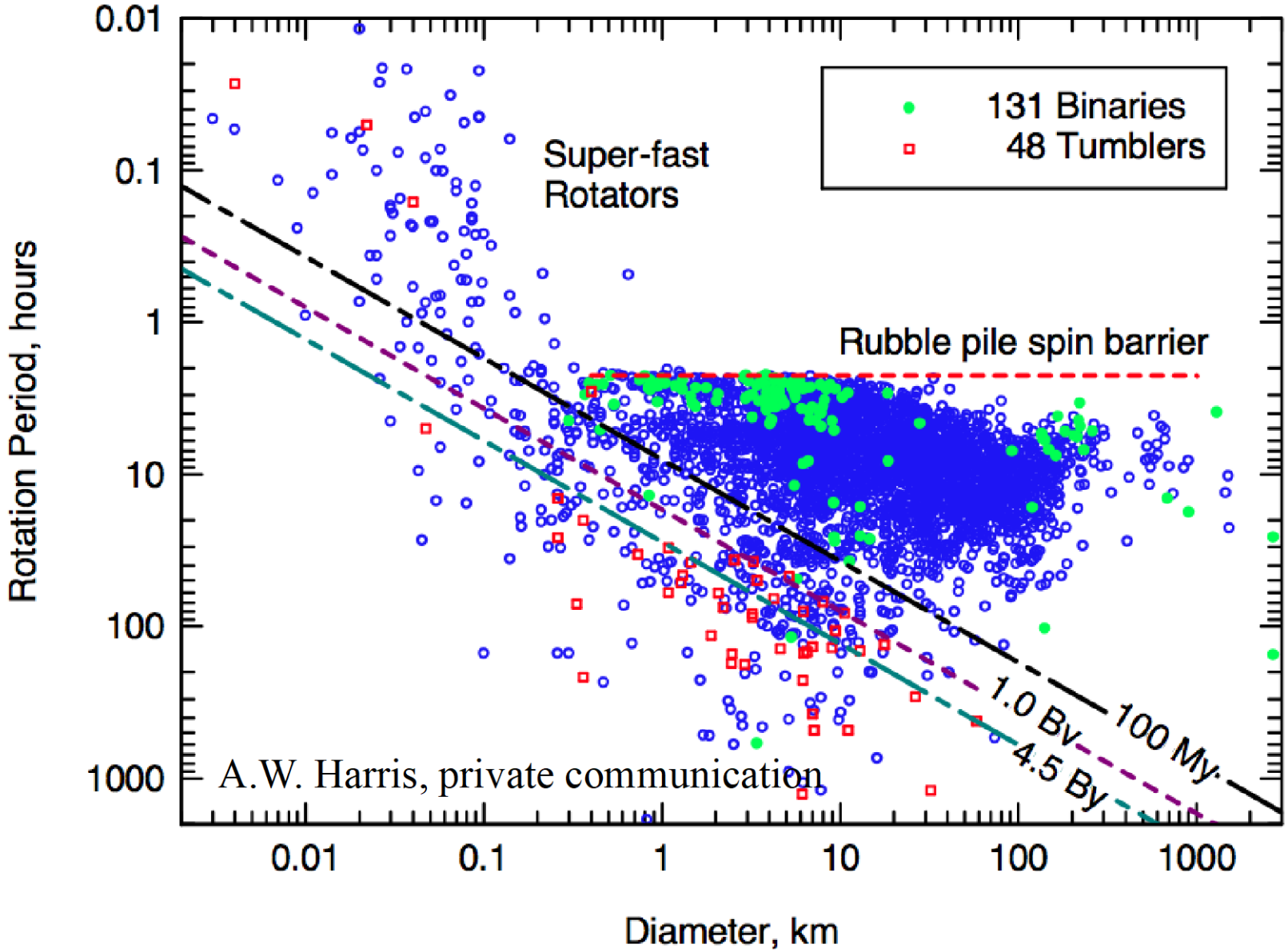

Pre-Decisional Information -- For Planning and Discussion Purposes Only
© 2016 California Institute of Technology. Government sponsorship acknowledged.

marco.b.quadrelli@jpl.nasa.gov

Itokawa size distribution

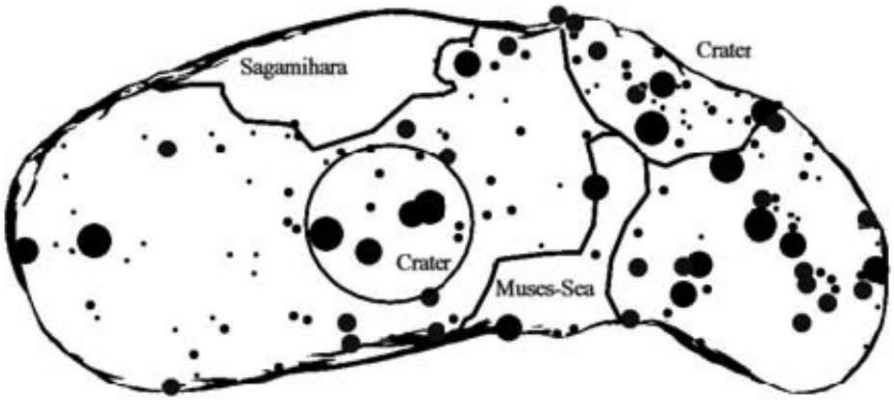

D.J. Scheeres, A. Richard Seebass Chair, University of Colorado at Boulder

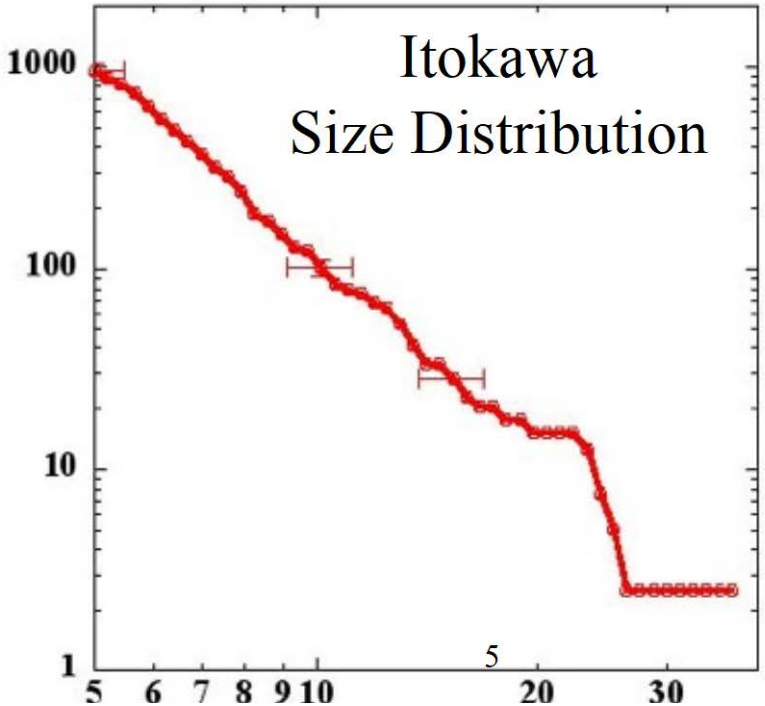

Pre-Decisional Information -- For Planning and Discussion Purposes Only
© 2016 California Institute of Technology. Government sponsorship acknowledged.

marco.b.quadrelli@jpl.nasa.gov

Forces vs. particle size

– **Gravity & Rotation**:

$$F_{gr} = m\left|\omega^2 r - g\right| = \frac{4\pi}{3} R^3 g_a$$

– **Friction**:

$$F_F = \mu\left[m g_a + F_{ng}\right]$$

On surface, controlled by ambient weight and non-gravitational forces

– **Electrostatics**:

$$F_{es} = C_{es} R^2$$

$$C_{es} = 10^{-8}, 10^{-1}$$

Transient, with max value for localized regions at the terminator

– **Solar Radiation Pressure**:

$$F_{srp} = C_{srp} R^2$$

$$C_{srp} = 10^{-5}/d^2$$

d = Asteroid distance from sun in AU

– **Cohesion (due to van der Waals attraction)**:

$$F_{vdw} = C_{vdw} R$$

$$C_{vdw} = 4 \times 10^{-2}$$

Derived for lunar regolith in (Perko et al. 2001)

D.J. Scheeres, A. Richard Seebass Chair, University of Colorado at Boulder

Pre-Decisional Information -- For Planning and Discussion Purposes Only
© 2016 California Institute of Technology. Government sponsorship acknowledged.

marco.b.quadrelli@jpl.nasa.gov

Comparison of Forces vs. sizes

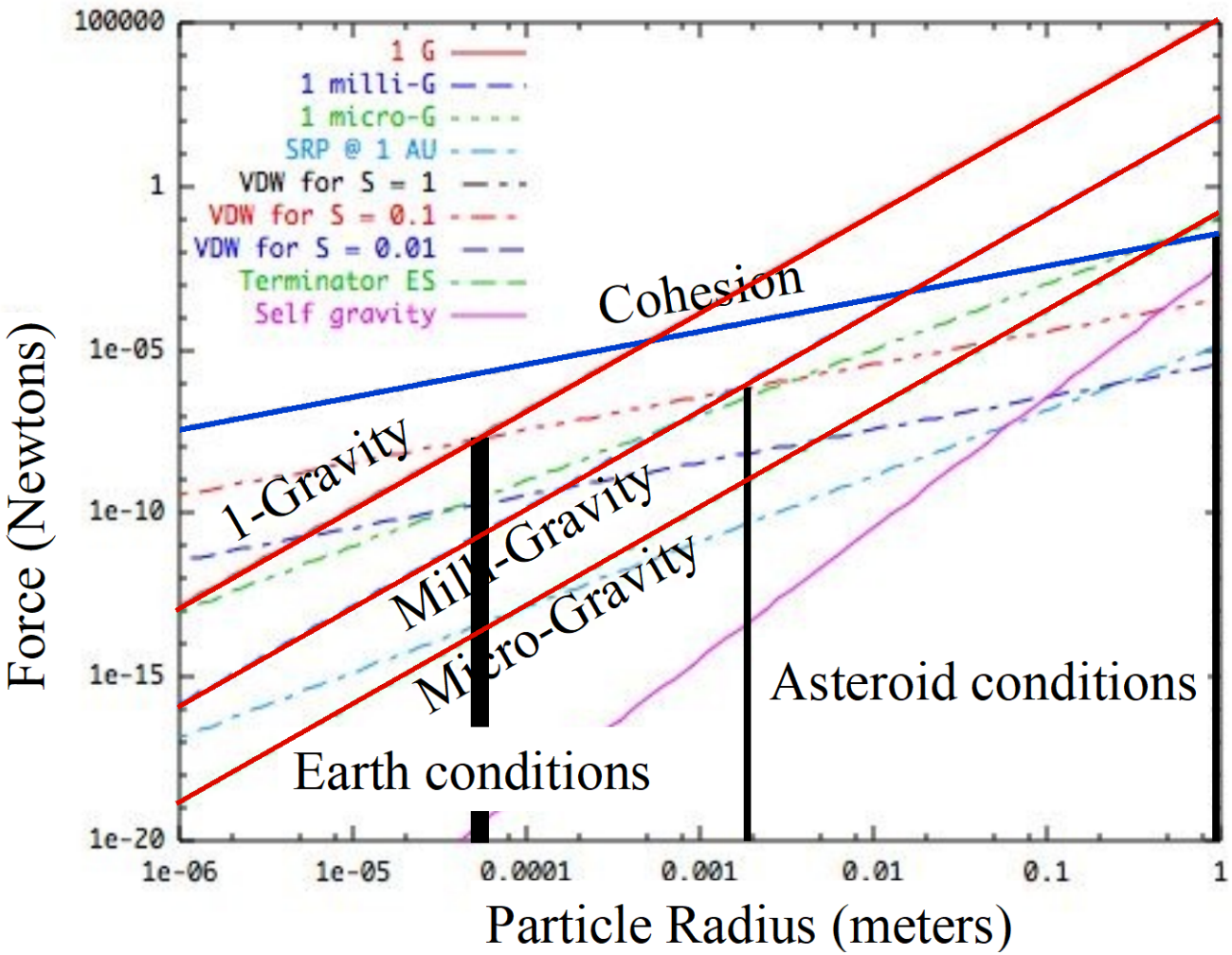

D.J. Scheeres, A. Richard Seebass Chair, University of Colorado at Boulder

Inter-particle cohesion forces are relevant for centimeter-sized particles in milli-G and larger particles in micro-G environments

Pre-Decisional Information -- For Planning and Discussion Purposes Only
© 2016 California Institute of Technology. Government sponsorship acknowledged.

marco.b.quadrelli@jpl.nasa.gov

Forces on a Small Body

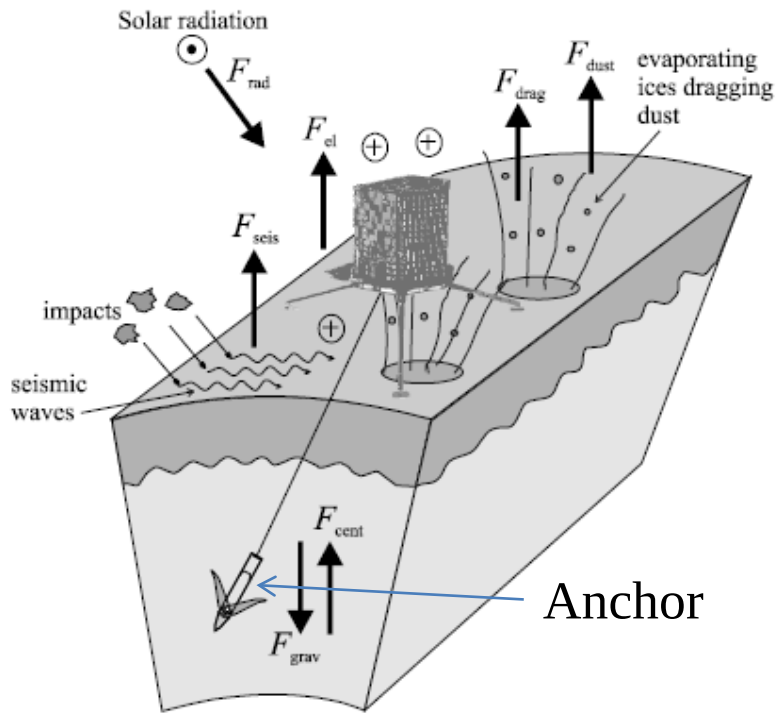

Figure 7.1. Schematic diagram of the *Rosetta Lander* on the surface of the comet nucleus, showing the main natural forces acting on the Lander (*RoLand* demonstration model photo: DLR).

Force	Direction
Weight of Lander	To center of mass of body
Centrifugal force	Outwards from rotation axis
Drag from evolved gas	Mostly radial, some tangential (wind)
Impact from dust	Complex flux (mostly radial)
Solar radiation	Anti-solar direction
Passage of seismic waves	Normal to surface
Reaction from lander moving	Depends on motion
Anchor cable	In tether tension

"Measuring Physical Properties at the Surface of a Comet Nucleus" Andrew J Ball, Ph.D thesis 1997, University of Kent, Canterbury, UK.

Pre-Decisional Information -- For Planning and Discussion Purposes Only
© 2016 California Institute of Technology. Government sponsorship acknowledged.
marco.b.quadrelli@jpl.nasa.gov

Forces on a Comet Lander

From Ball's thesis

Force	Direction(s)	Magnitude
Weight of the lander (gravitational force)	Towards centre of mass of nucleus	$F_{grav} = M \cdot \frac{4}{3}\pi R_c \rho_c G$
Centrifugal force	Outwards from nucleus rotation axis	$F_{cent} = M \cdot \frac{4\pi^2 R_c \cos\delta}{P^2}$
Drag from evolved gas	Mostly radial away from nucleus, possibly some tangential component (wind)	$F_{drag} = 4R^2 C_D a e^{-\frac{b}{T}}$
Impact of dust particles	Complex (mostly radial) flux, partially coupled to gas flow	F_{dust} = momentum transferred per unit time; related to gas flow

Pre-Decisional Information -- For Planning and Discussion Purposes Only
© 2016 California Institute of Technology. Government sponsorship acknowledged.

marco.b.quadrelli@jpl.nasa.gov

Forces on a Comet Lander

From Ball's thesis

Force	Direction(s)	Magnitude
Solar radiation	Anti-solar direction (day only)	$F_{\mathrm{rad}} = \frac{\pi R^2}{c} \cdot \frac{1371\,[\mathrm{Wm}^{-2}]}{(d\,[\mathrm{AU}])^2}$
Passage of seismic waves	Many	$F_{seis} = \frac{4\pi^2 M z_0}{\tau^2}$
Electrostatic	Normal to nucleus surface (repulsive)	$F_{\mathrm{el}} = \pi R^2 \cdot \frac{e n_e \Phi_s}{2}$
Reaction from moving parts (e.g. drill & deployable experiments)	Many (upwards for devices lowered to surface or drilling into it)	F_{reac} = mass of moving part × velocity / acceleration time
Anchor cable tension	Downwards	F_{anc}, determined by harpoon rewind motor

Pre-Decisional Information -- For Planning and Discussion Purposes Only
© 2016 California Institute of Technology. Government sponsorship acknowledged.

marco.b.quadrelli@jpl.nasa.gov

Forces on a Small Body – cont.

- Anchoring force should overcome other forces acting on lander
- Minimum anchoring force needed:
  75 kg lander - 10N anchor force
  750 kg lander - 100N anchor force
- More forces needed to resist forces during activities such as drilling, coring, sampling.

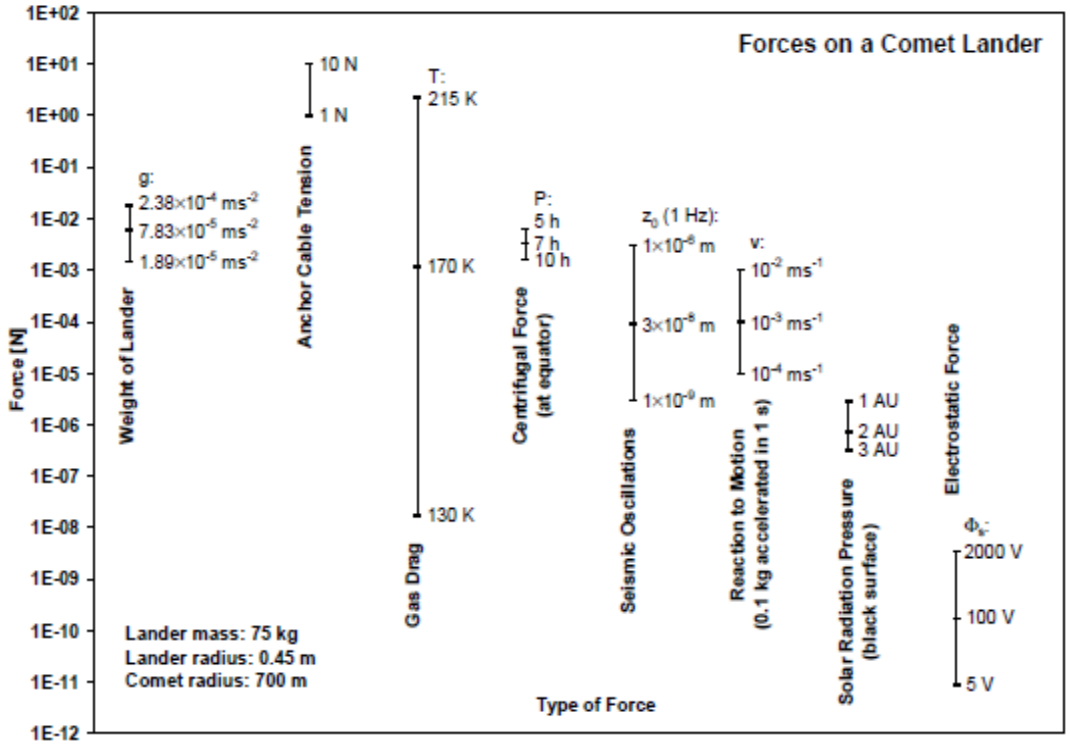

Figure 7.2. Comparison of the various forces acting on the Lander, based on the calculations in the text.

"Measuring Physical Properties at the Surface of a Comet Nucleus" Andrew J Ball, Ph.D thesis 1997, University of Kent, Canterbury, UK.

Pre-Decisional Information -- For Planning and Discussion Purposes Only
© 2016 California Institute of Technology. Government sponsorship acknowledged.
marco.b.quadrelli@jpl.nasa.gov

Ionocraft

http://starwars.wikia.com/wiki/X-34_landspeeder

The Ionocraft, patented by Major Alexander P. de Seversky, is propelled by the emission of ions. It may eventually be used as a TV relay station or missle destroyer. The downward flow of smoke shows the powerful electrostatic down draft created by the vehicle.

1296 square inches, 2 oz. weight
constructed of about $5.00 worth of
balsa wood and aluminum wire
consumes 90 watts of electricity
(30,000 volts X .003 amps)

Power-to-weight ratios IonoCraft .96 hp/lb
Piper Cub .065 hp/lb helicopter .1 hp/lb

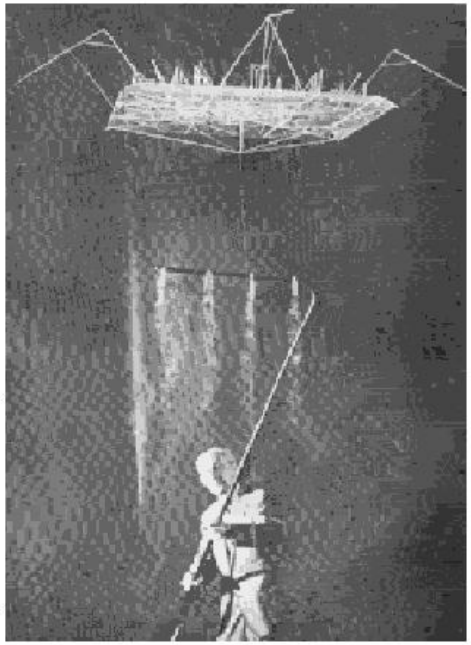

http://starwars.wikia.com/wiki/X-34_landspeeder

Pre-Decisional Information -- For Planning and Discussion Purposes Only
© 2016 California Institute of Technology. Government sponsorship acknowledged.

marco.b.quadrelli@jpl.nasa.gov

JPL Integrated Modeling and Simulation for Primitive Body Sampling

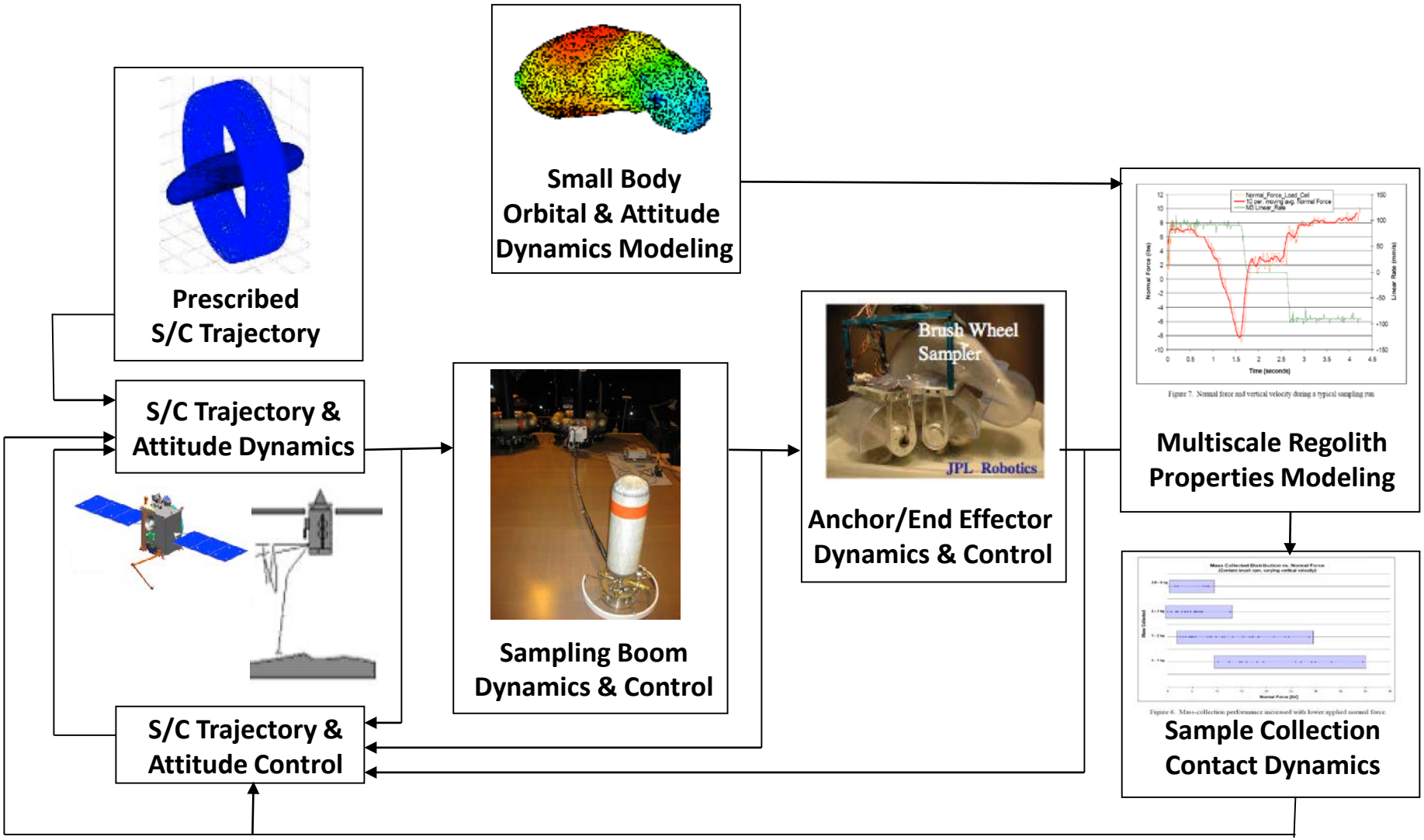

Pre-Decisional Information -- For Planning and Discussion Purposes Only
© 2016 California Institute of Technology. Government sponsorship acknowledged.

marco.b.quadrelli@jpl.nasa.gov

Asteroid surface charging

The environment near the surface of airless bodies (asteroids, comets, Moon) is electrically charged due to interactions with the solar wind plasma and UV radiation.
Charged dust is ever present, in the form of dusty plasma [Vladimirov]. Comets have a gas tail and a second electrostatic tail. This environment is also largely unexplored.

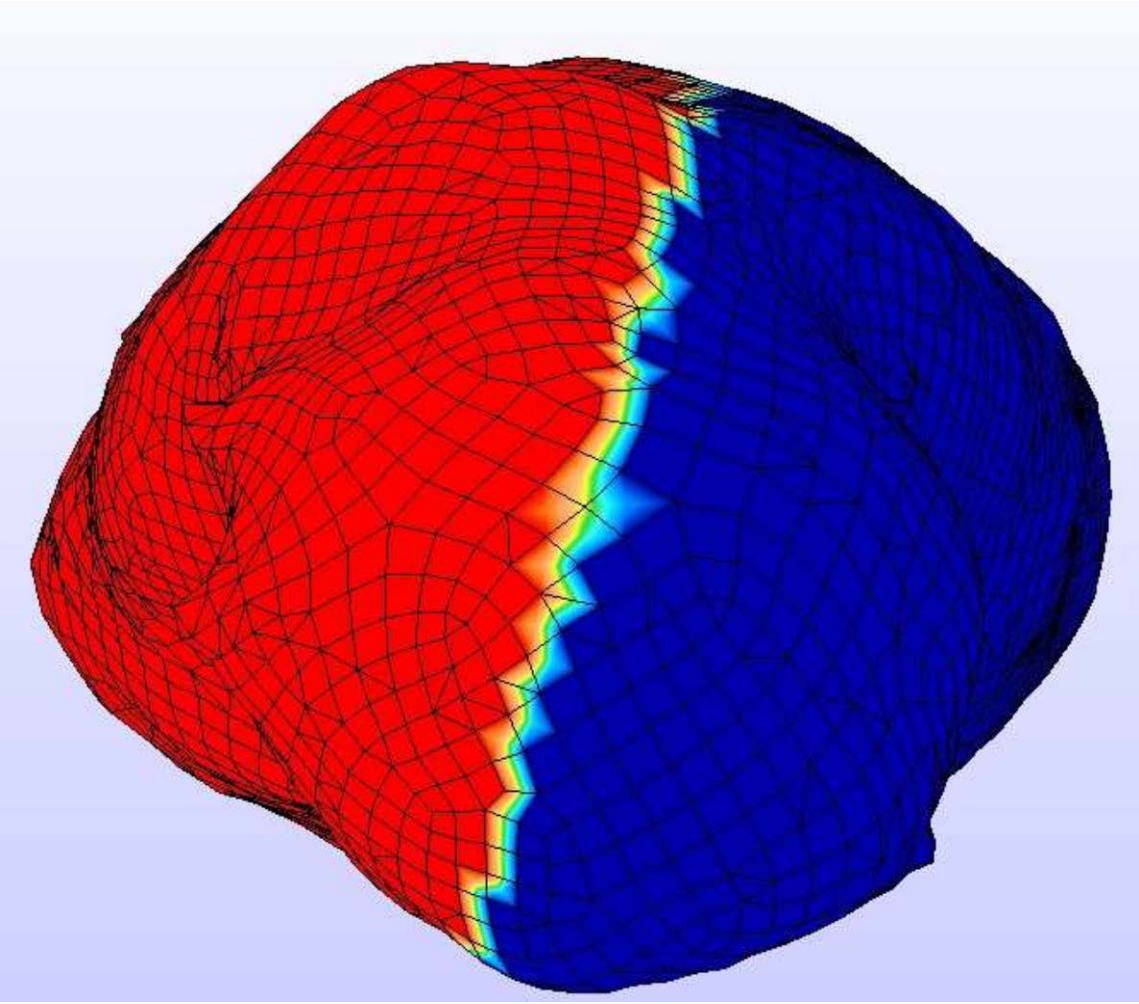

Pre-Decisional Information -- For Planning and Discussion Purposes Only
© 2016 California Institute of Technology. Government sponsorship acknowledged.

marco.b.quadrelli@jpl.nasa.gov

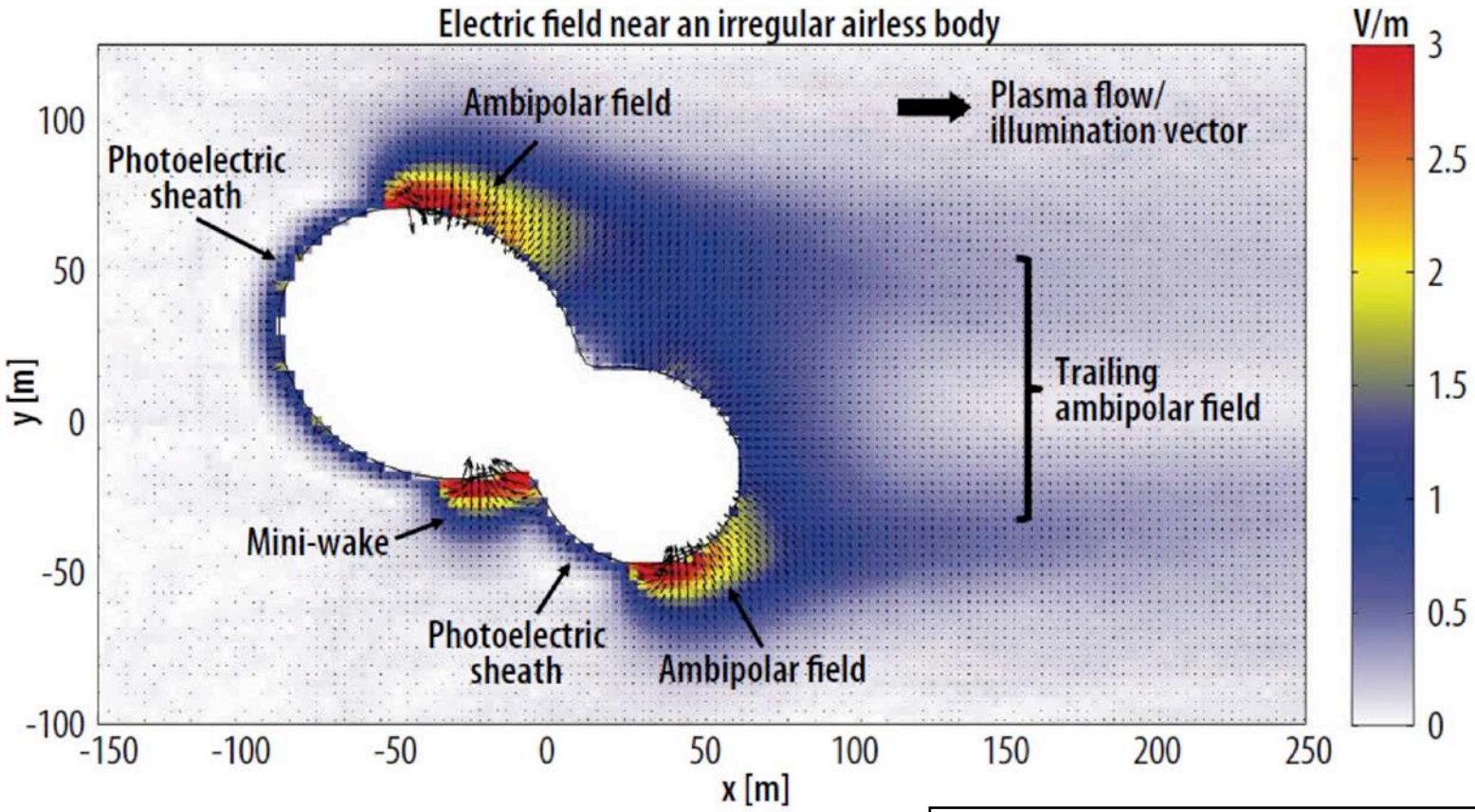

Simulated interaction of the solar wind with a small irregularly shaped asteroid, about 150 meters long by 50 meters wide (roughly 164 yards by 55 yards).
The deepest shades of red indicate strong and possibly hazardous electric fields.
Credit: M.I. Zimmerman/W.M. Farrell/A.R. Poppe,
https://www.youtube.com/watch?v=bSXxaL9Hvvc

© 2016 California Institute of Technology. Government sponsorship acknowledged.
marco.b.quadrelli@jpl.nasa.gov

Charging environment

If a body with high surface resistivity is exposed to the solar wind and solar radiation, sun-exposed areas and shadowed areas become differentially charged.

Charging on the dayside surface is dominated by photoelectrons emitted due to solar UV radiation that create a positive surface potential, while the shadowed side accumulates electrons and acquires a negative surface potential.

Recent work [Kok] shows that, on the Moon, soft solar X-rays with wavelengths smaller than 25 Å can remove electrons with energies of 500 to 1500 eV from the surface and create cm-scale electric fields which may reach levels of ~50-150 kV/m.

Asteroid electric charge has never been measured, but simple estimates predict that an electric potential (~1 kV) can be attained on the dark side compared to the sunlit side, which becomes slightly positively charged by photoelectron emission. These differences are enhanced further at the terminator (the day/night boundary), when fields could reach ~100-300 kV/m [Aplin].

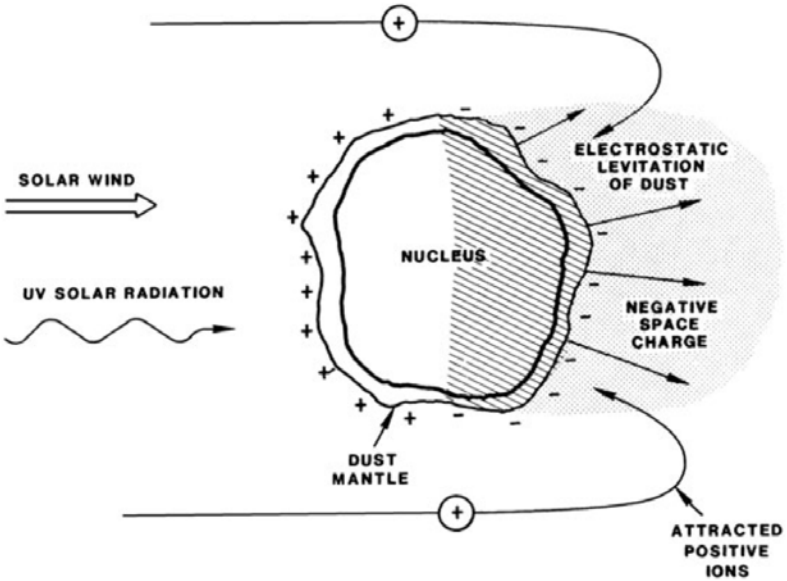

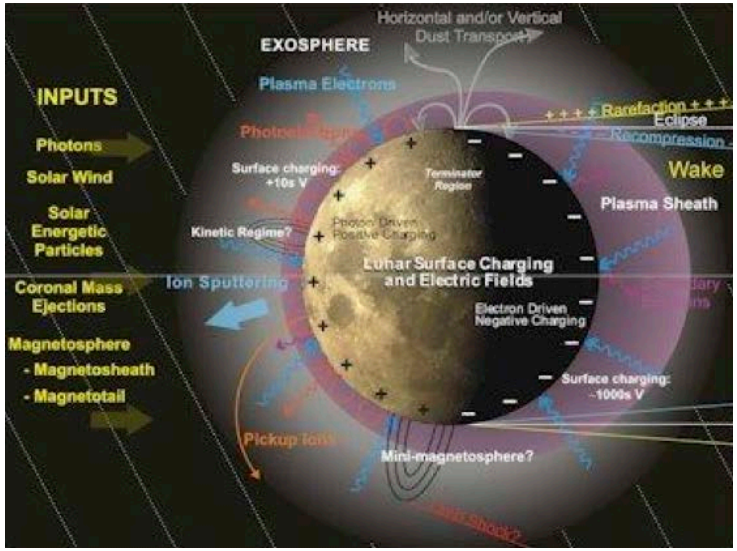

Pre-Decisional Information -- For Planning and Discussion Purposes Only
© 2016 California Institute of Technology. Government sponsorship acknowledged.

marco.b.quadrelli@jpl.nasa.gov

Charged dust levitation

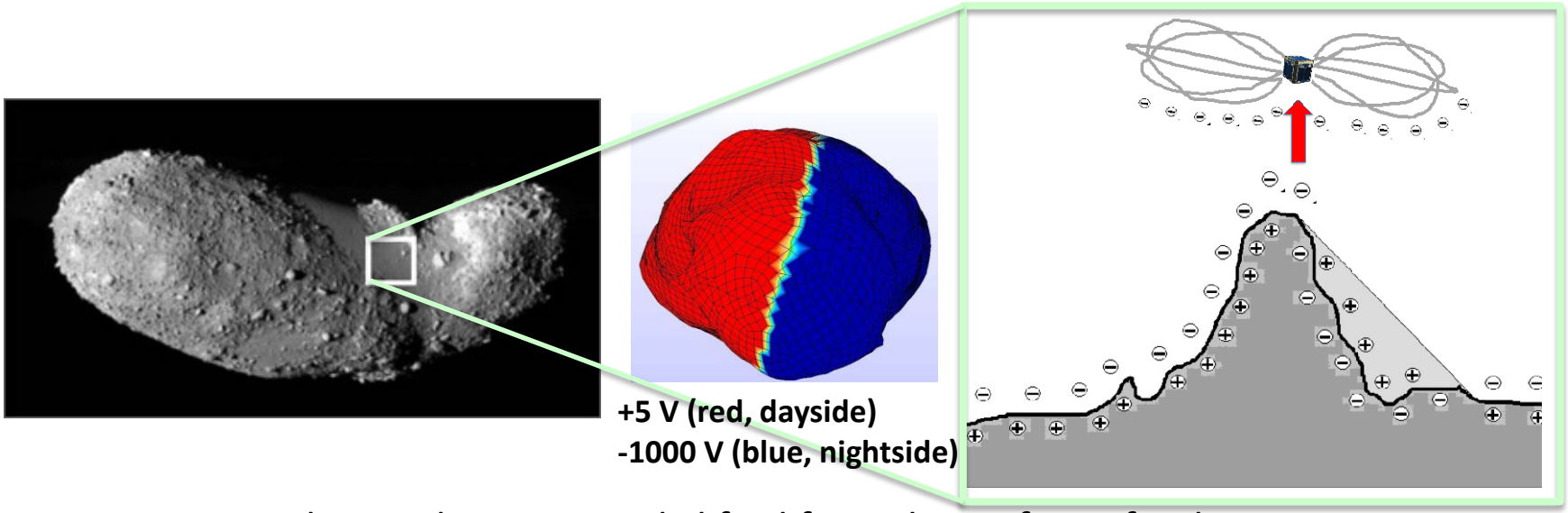

Millimeter-size particles can be most easily lifted from the surface of Itokawa [Hartzell2011]. As these particles are lifted, they dislodge smaller particles that are harder to lift due to their strong cohesive forces [Hartzell2013]. Once separated from the surface, grains can either travel on ballistic trajectories, escape from the asteroid, or levitate. During these migrations the larger particles can get trapped in topographic lows, as observed in [Miyamoto]. As a surface element on a resistive asteroid rotates into and out of view of the sun, electrostatic levitation may agitate its uppermost particulate layer. Larger levitated particles remaining gravitationally bound to the asteroid are redistributed across its surface following local electrostatic and gravity gradients.

Consequently, the study of levitating dust is relevant in that it provides some insight into the plasma environment and confirms the possibility of levitation.

Pre-Decisional Information -- For Planning and Discussion Purposes Only
© 2016 California Institute of Technology. Government sponsorship acknowledged.

marco.b.quadrelli@jpl.nasa.gov

Electric field strength to levitate

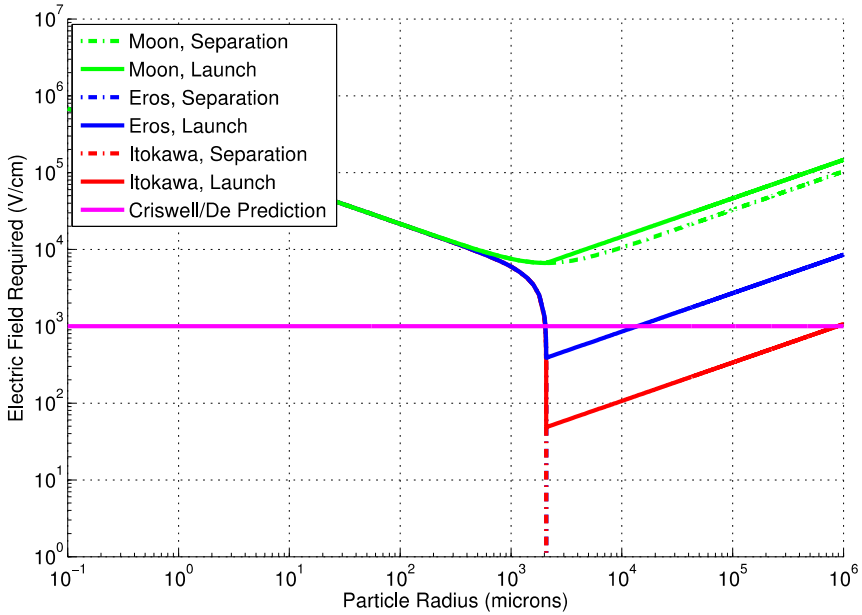

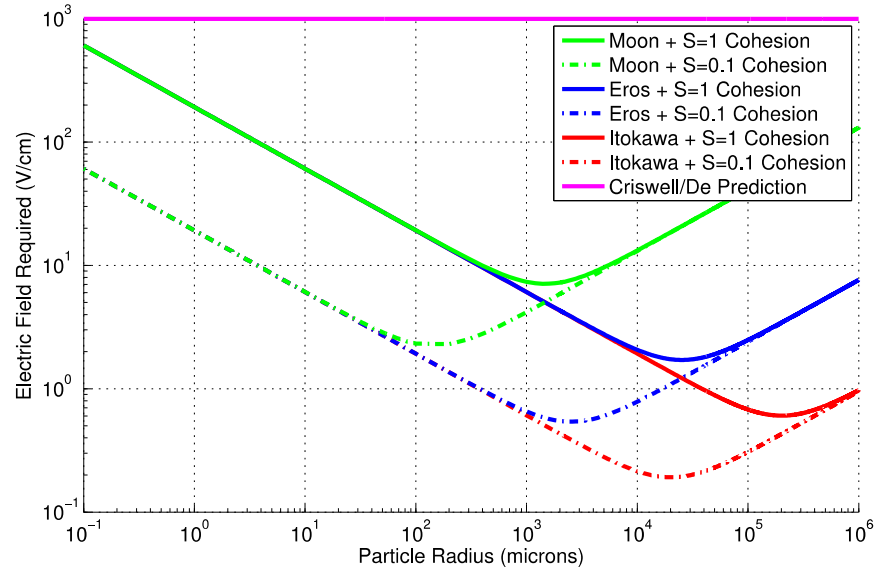

Electric field strength required to launch (or separate) spherical particles with a density of 3.5 g/cm^3 and S = 1 off lunar and asteroid surfaces with seismic accelerations of 0.5GL (GL is lunar gravity, 1.622 m/s^2).

Electric field strength required to electrostatically loft spherical particles with a density of 3.5 g/cm3 assuming a charge amplification ratio of 1.25×10^6, which is within the range that has been seen in experimentation. The bodies are assumed to be seismically quiet.

Courtesy of Christine Hartzell, UMD

Pre-Decisional Information -- For Planning and Discussion Purposes Only
© 2016 California Institute of Technology. Government sponsorship acknowledged.

marco.b.quadrelli@jpl.nasa.gov

Forces of different origin act on charged body in space

In space, behavior depends on the dynamic balance of:

- Solar radiation pressure,
- Gravitational forces,
- Electrostatic forces,
- Lorentz forces,
- Cloud self-gravity,
- Poynting-Robertson drag,
- Yarkovsky effect.

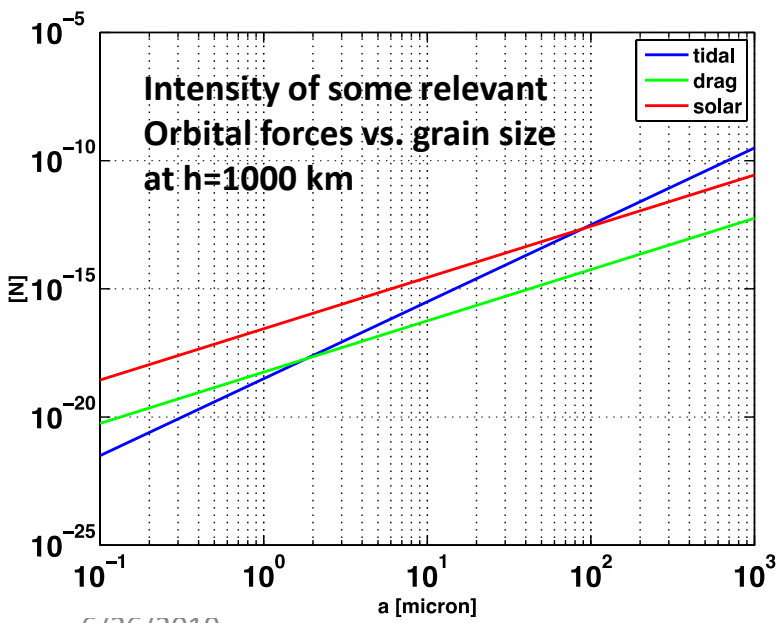

Force	Expression	Relevance
Gravity	$m_d g = (4\pi/3)a^3 \rho g$	Can be used to align cloud.
Electromagnetic	$Q_d E$	Can be used to levitate dust.
Neutral drag	$u_d >> v_T$ $\quad F_{nd} = \pi a^2 \rho_g m_n u_d^2$ $u_d << v_T$ $\quad F_{nd} = m_d u_d \left(\delta \frac{8\sqrt{\pi}}{3} a^2 \rho_g \frac{m_g}{m_d} v_T \right)$	Dissipative.
Thermophoretic	$F_{th} = \frac{4\sqrt{2\pi}}{15} \frac{a^2}{v_T} \kappa \nabla T$	*Arises if there is a temperature gradient in the neutral gas. It is due to the asymmetry in the momentum transfer to dust from neutrals and is directed toward lower gas temperatures. This force can be used to levitate particles against gravity.*
Ion drag	$F_{id} = n_i m_i u_i u_s \pi \left(b_c^2 + 4\Lambda b_{\pi/2}^2 \right)$	*Arises from the momentum transfer from flowing ions to charged microparticles in a plasma. Sum of* collection force due to ions impinging on grain and orbit force due to ions deflected by graiins.

u_d = dust velocity, v_T = gas thermal speed, ρ = grain density, ρ_g = gas density, δ=scattering coeff., κ=thermal conductivity of gas, u_i=ion drift speed, u_s=mean ion speed, b_c=collision impact parameter, b_{90}=impact parameter for 90 deg. Collisions, Λ=function of Debye length and collision parameters.

Pre-Decisional Information -- For Planning and Discussion Purposes Only
© 2016 California Institute of Technology. Government sponsorship acknowledged.

marco.b.quadrelli@jpl.nasa.gov

Analogs in Nature

- observed "unaccountable rapidity" in the launching of ballooning spiders from the vessel H.M.S. Beagle, recorded by Charles Darwin during his famous voyage, on a day without wind, and far away from the shore.
- It is believed that such spiders are able to emit threads that are either pre-loaded with a static electric charge, so that the presence of this charge will lead both to mutual repulsion among the emitted threads, and an additional overall induced electrostatic force on the spider, providing a component of lift that is independent of convection or aerodynamic effects.

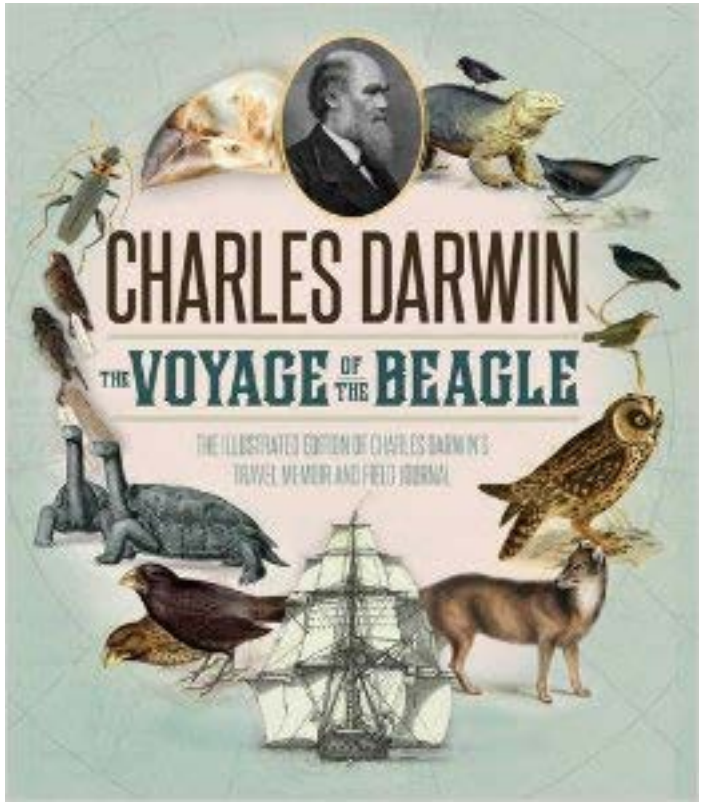

Electrostatic properties
Of spider silk

www.oxfordsilkgroup.com

The E-Glider biomorphically behaves like one of these spiders, greatly favored by the charged environment, in absence of aerodynamics and convection, and in the microgravity fields at small bodies.

Pre-Decisional Information -- For Planning and Discussion Purposes Only
© 2016 California Institute of Technology. Government sponsorship acknowledged.

marco.b.quadrelli@jpl.nasa.gov

Ballooning spiders

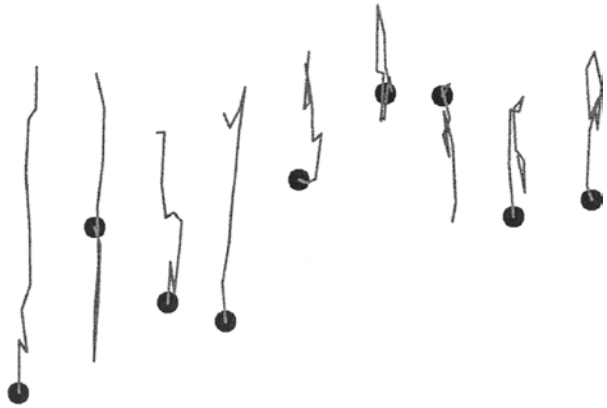

flight pattern of a
ballooner and dragline

Gorham refers to existing observations and the physics of spider silk in the presence of the Earth's static atmospheric electric field (-120 V/m negative) to indicate a potentially important role for electrostatic forces in the flight of Gossamer spiders.

Source: http://arxiv.org/abs/1309.4731

Pre-Decisional Information -- For Planning and Discussion Purposes Only
© 2016 California Institute of Technology. Government sponsorship acknowledged.

marco.b.quadrelli@jpl.nasa.gov

Previous Small Body Landers and Orbiters

- Landers:
  - DAS (Phobos 1 & 2, failed)
  - PROP-F (Phobos 2, failed)
  - MINERVA (MUSES-C/Hayabusa, failed)
  - MUSES-CN (Cancelled)
  - Philae (Rosetta)
  - MASCOT (Hayabusa 2, en route)
  - Phobos-Grunt (failed)
- Orbiters
  - NEAR Shoemaker (unplanned lander)
  - Deep Impact (hard lander)
  - OSIRIS-Rex (fly-by and sample, launch fall '16)

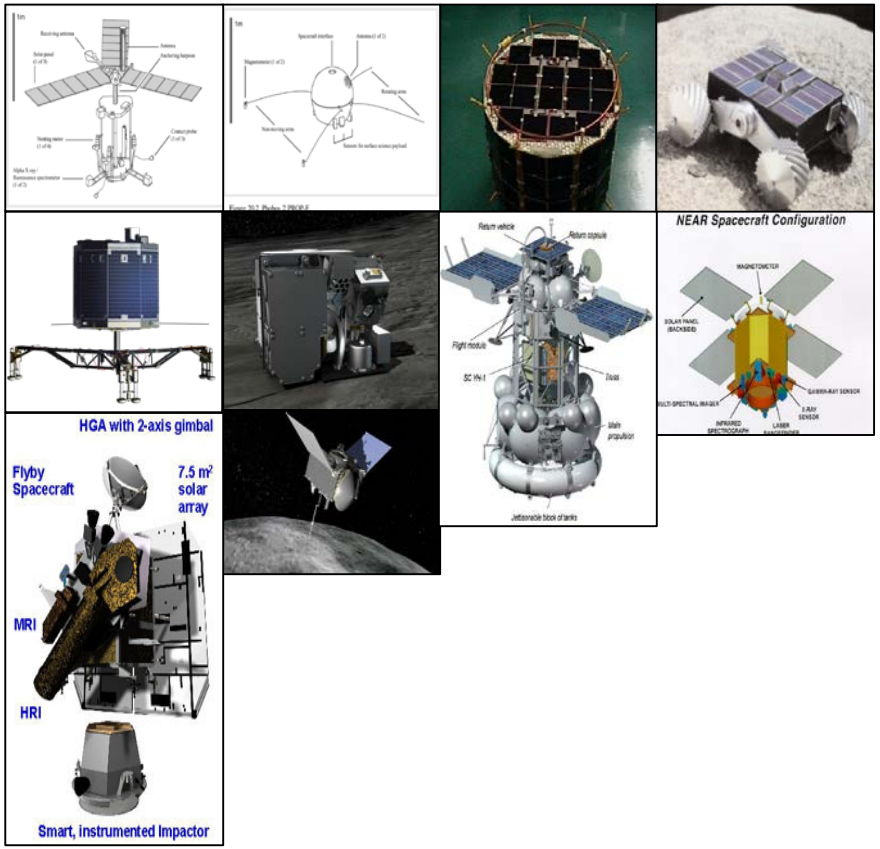

Pre-Decisional Information -- For Planning and Discussion Purposes Only
© 2016 California Institute of Technology. Government sponsorship acknowledged.

marco.b.quadrelli@jpl.nasa.gov

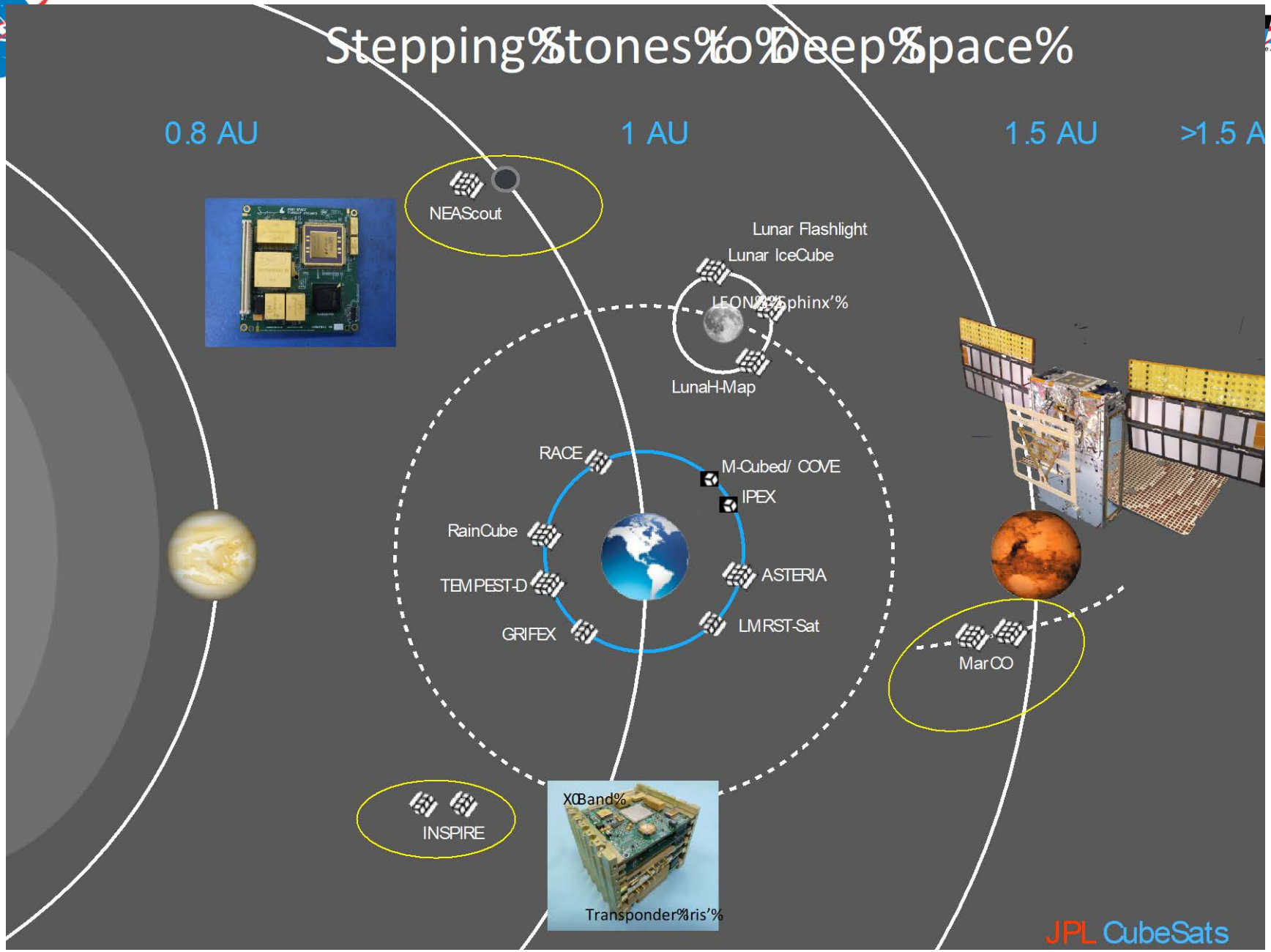

Courtesy of Julie Castillo-Rogez, JPL

Pre-Decisional Information -- For Planning and Discussion Purposes Only
© 2016 California Institute of Technology. Government sponsorship acknowledged.

marco.b.quadrelli@jpl.nasa.gov

Science Objectives at NEOs (Examples)

Objectives	Observations	Measurements	Architecture
Determine surface mechanical properties	Soil competence, granularity at all scales, gravity	High resolution imaging, gradiometer, mechanical tester	Reconnaissance with orbiter, track rover's motion and interaction with dust
Search for in-situ resources	Chemical and mineralogical composition	NIR, GRaND, APXS	Remote sensing from orbiter, in-situ characterization at selected sites
Characterize risk and search for mitigation approaches	Waves and fields (e.g., electrostatic field), dust dynamics	UV imaging, high-res imaging	In situ
Understand and simulate human activities in low-gravity environment	Simulate digging, sampling	Performance	In situ

Courtesy of Julie Castillo-Rogez, JPL

Pre-Decisional Information -- For Planning and Discussion Purposes Only
© 2016 California Institute of Technology. Government sponsorship acknowledged.

marco.b.quadrelli@jpl.nasa.gov

Decadal Science Mapping and Instrument Availability

THEME	MEASUREMENTS	OPPORTUNITY FOR CUBESAT/SMALLSAT	INSTRUMENTS
Building New Worlds	Isotopic, elemental, mineralogical composition	In situ, extreme environments	APXS, TLS, IR Spec, Submm Spec, UV Spec, Gamma Ray/NeutronSpec, Dust Spec, MassSpec
		Returned sample (small bodies)	Sample Return Capsule (possibly Acquisition as well)
Planetary Habitats Ocean Worlds	Composition (volatiles, organics) endogenic activity, heat budget, environment	In situ	MassSpec, Micro-XRF, Imaging, IR Spec, Seismometer, heat probe, radar
Processes	Atmospheric structure, fields, plasma, dust	Close proximity, in situ, multiple data points	Imaging, IR Spec, Mag, Transponders, Langmuir probes, Mass Spec, TLS, Plasma Spec.
Human Exploration	Dust, fields, radiations, Gravity field, orbital properties Regolith mechanical properties ISRU (composition)	Close proximity, in situ, risky environments	Dust Counter, Neutron, Geophysics Inst., IR Spec, APXS, Transponders, radiations spec, Surface perturbation, radar, seismometer

Color code: Green = exists; Blue = in development; Red = does not exist yet

Courtesy of Julie Castillo-Rogez, JPL

Pre-Decisional Information -- For Planning and Discussion Purposes Only
© 2016 California Institute of Technology. Government sponsorship acknowledged.

marco.b.quadrelli@jpl.nasa.gov

BioSentinel Radiation "Spectrometer"

- Teaming with JSC's **RadWorks Project** for integrated radiation sensor/spectrometer
- Radiation Environment Monitor (REM)
  - compact, low-power detector based on novel hybrid pixel sensor (Medipix2 / Timepix from CERN; 256 x 256 pixels)
  - provides dose, LET (linear energy transfer), and coarse particle segregation per event
  - 5 are currently deployed on ISS: *high TRL*
- REM advanced miniaturized design can readily be integrated into Nanosatellite BioSentinel payload architecture
- Potential alignment of sensor to correlate specific events with growth of yeast in specific microwells
- Forward work: Requirements, Schedule, Funding, Implementation plan
- B.G. Swan and E. Semones leading & interfacing w/ ARC

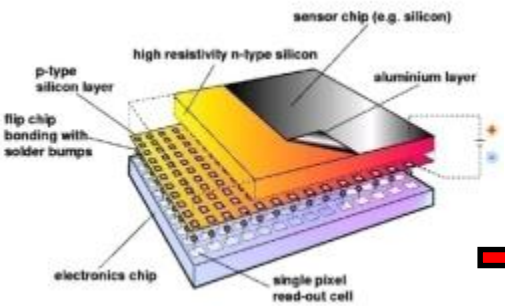

Technology

Prototype

SDTO Development Unit

Packaged Unit
- < 150 g
- 10 x 20 x 60 mm
- USB Interface

Courtesy of Julie Castillo-Rogez, JPL

Pre-Decisional Information -- For Planning and Discussion Purposes Only
© 2016 California Institute of Technology. Government sponsorship acknowledged.

marco.b.quadrelli@jpl.nasa.gov

New Science Grade Instrument Capabilities

QIT-MS
JPL

Quadrupole Ion Trap Mass Spectrometer

2.5 kg, 2U, isotopic accuracy <1%, leverages foldable edge-connected electronics

SWIS
JPL

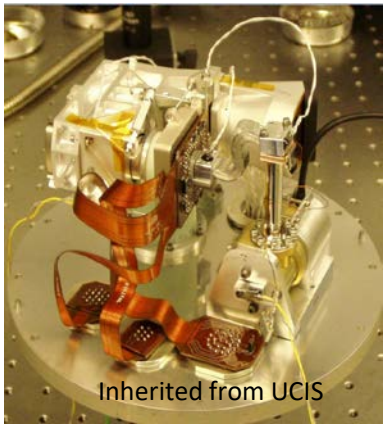

Snow and Water Imaging Spectroscopy

High-throughput, low-polarization, high-uniformity spectrometer, 350-1700 nm spectral range

HOT-BIRD
JPL

Advanced Infra-Red Photodetector

Thermal sensitivity of 0.2 deg, funded for infusion on CIRAS

IntelliCam
JPL

High-Resolution Visible Camera

Used for science, optical navigation, and Autonomous Navigation demonstration

Courtesy of Julie Castillo-Rogez, JPL

© 2016 California Institute of Technology. Government sponsorship acknowledged.

marco.b.quadrelli@jpl.nasa.gov

Other Instrumentation

Broadband MEMS-based Seismometer

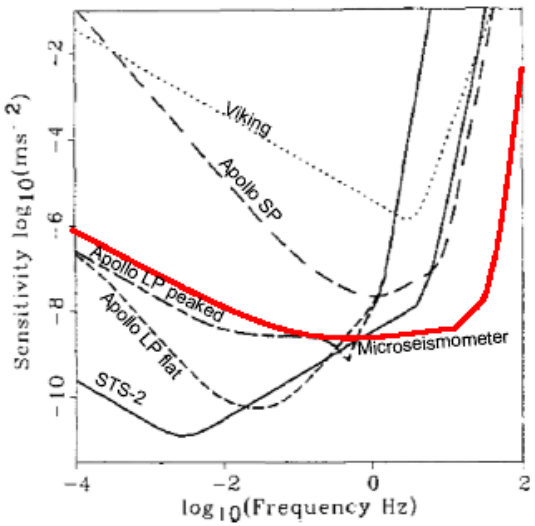

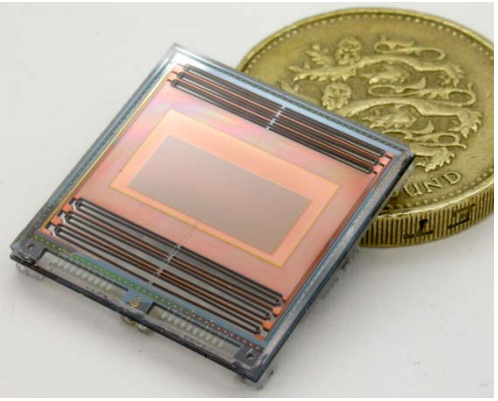

Micro-seismometer
Imperial College, London

Intelligent UV Fluorescence Microscope

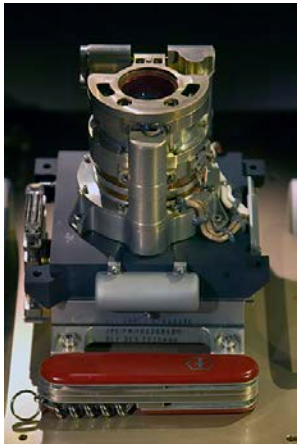

e.g., MSL's MAHLI, expand on UV LED concept or with laser addition

Technique well studied for organic search; developed for JPL's Cryobot and ESA's LIFE's instrument (PanCam updated with 365 nm light emitting diode or 375 nm laser source)

Example UV laser diode (right) and circuitry (left)

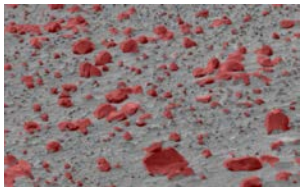

Analysis of Mars surface D. Thompson's Intellicam software; focused data extraction can reduce data volume by 3-4 orders of magnitude

Instrument / Parameter	Mass (g)	Volume (l)	Power (W)	Integration Time (sec)	Data Volume (kb)
Seismometer	300	~0.01	0.1-0.2	< 1 min.	1-10 kb after wavelet compression
UV Microscope	200	0.25	1.8-2.4	< 1sec.	~10-100kb per image after on-board analysis

Other instruments are possible (e.g., radiation monitor, thermometers, etc.)

Courtesy of Julie Castillo-Rogez, JPL

Pre-Decisional Information -- For Planning and Discussion Purposes Only
© 2016 California Institute of Technology. Government sponsorship acknowledged.

marco.b.quadrelli@jpl.nasa.gov

Science Grade Instruments are getting smaller

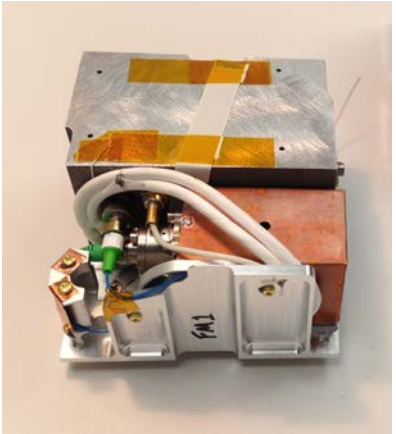

INSPIRE Vector Helium Magnetometer (0.4U) (as good as Cassini)

Miniature Quadrupole Ion Trap Mass Spectrometer with 100x higher sensitivity - JPL Prototype

Deep Space Camera (5 megapixel) Malin Space Science Systems http://www.msss.com/brochures/c50.pdf

Courtesy of Julie Castillo-Rogez, JPL

Pre-Decisional Information -- For Planning and Discussion Purposes Only
© 2016 California Institute of Technology. Government sponsorship acknowledged.

marco.b.quadrelli@jpl.nasa.gov

Many Small Instruments are Inherited from Deep Space Missions

ELEMENTS/ISOTOPES	MINERALOGY	GEOLOGY	GEOPHYSICS	ENVIRONMENT

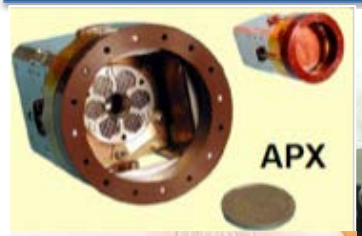

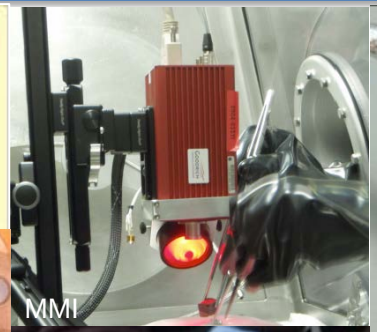

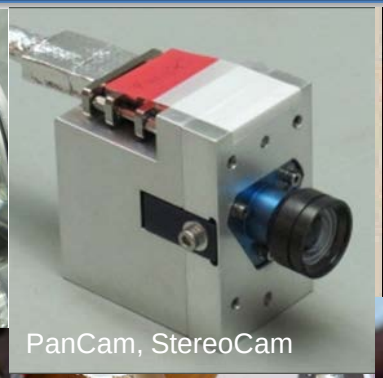

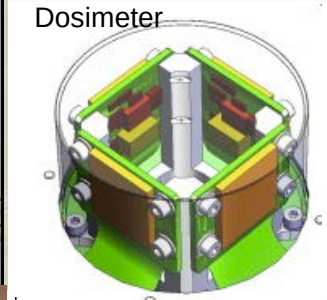

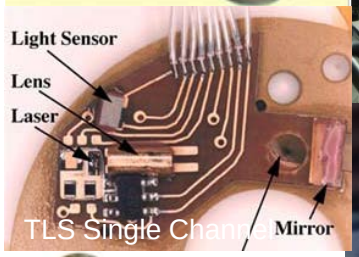

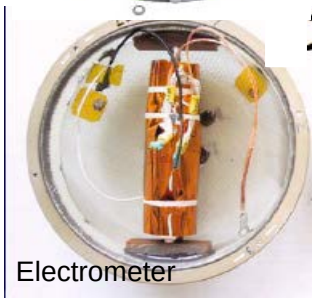

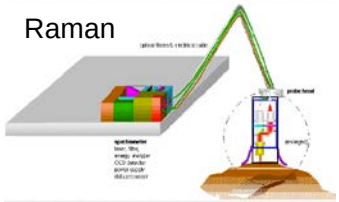

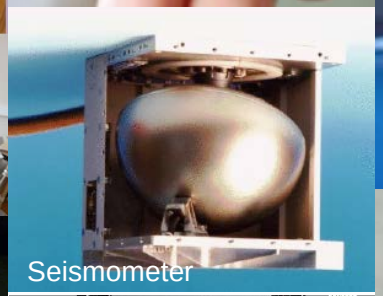

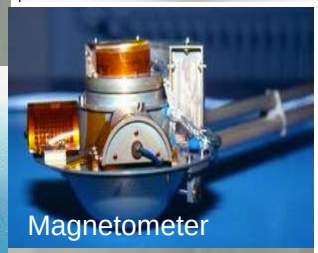

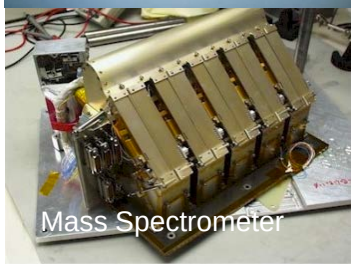

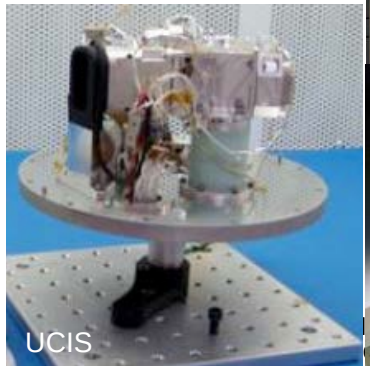

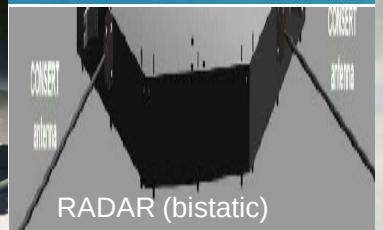

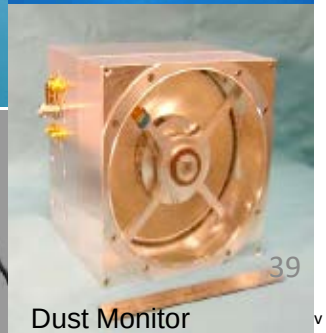

Debye Shielded Force

In a plasma environment, an oppositely charged sheath forms about a charged space object.

The electron Debye Length is defined as: $\lambda_D = \sqrt{\frac{\epsilon_0 \kappa T_e}{n_e e_c^2}},$

Assuming the object's potential is is small compared to the plasma temperature, the potential about a sphere drops off as:[1,2]

$$\Phi(r) = \frac{V_A R_A}{r} e^{-(r-R_A)/\lambda_D}.$$

The E-field is the gradient of the potential, and is expressed as:

$$E(r) = -\nabla_r \Phi(r) = \frac{V_A R_A}{r^2} e^{-(r-R_A)/\lambda_D} \left(1 + \frac{r}{\lambda_D}\right)$$

The Debye Shielding increases the local gradient of the potential, and thus can increase the capacitance of the surface. This can yield a strong E field, thus force, near a surface, but at some distance the shielding dominates.[2]

$$F = \frac{V_A R_A q_B}{d^2} e^{-(d-R_A)/\lambda_D} \left(1 + \frac{d}{\lambda_D}\right)$$

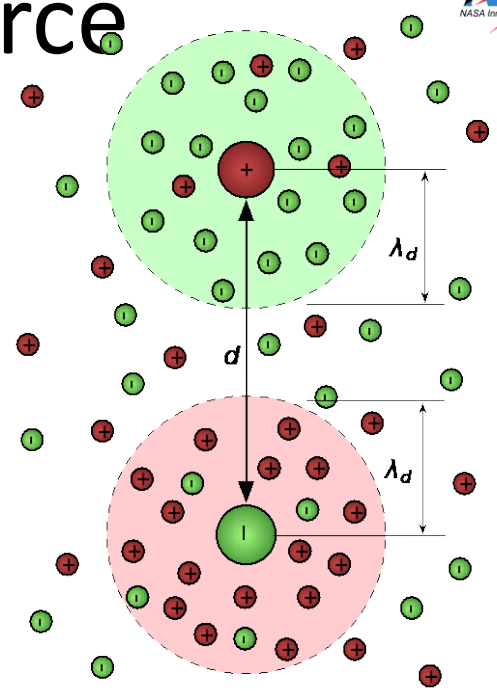

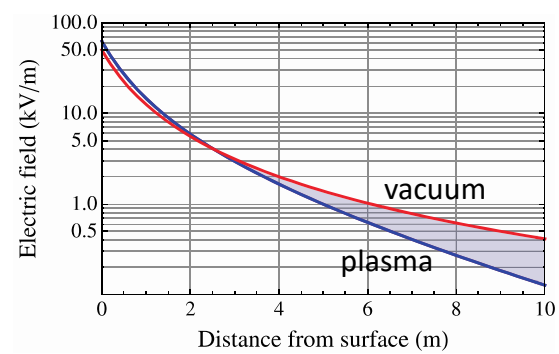

1m diameter sphere with λ=4m

[1]Whipple, E. C., "Potentials on Surfaces in Space," Rep. Prog. Phys, Vol. 44, No. 11, 1981, pp. 1197–1250.
[2]C. R. Seubert, L. A. Stiles and H. Schaub, "Effective Coulomb Force Modeling For Spacecraft In Earth Orbit Plasmas," *Advances in Space Research*, Vol. 54, No. 2, 2014, pp. 209–220. doi:10.1016/j.asr.2014.04.005

Courtesy of Hanspeter Schaub, UC Boulder

Pre-Decisional Information -- For Planning and Discussion Purposes Only
© 2016 California Institute of Technology. Government sponsorship acknowledged.

marco.b.quadrelli@jpl.nasa.gov

Forces at play

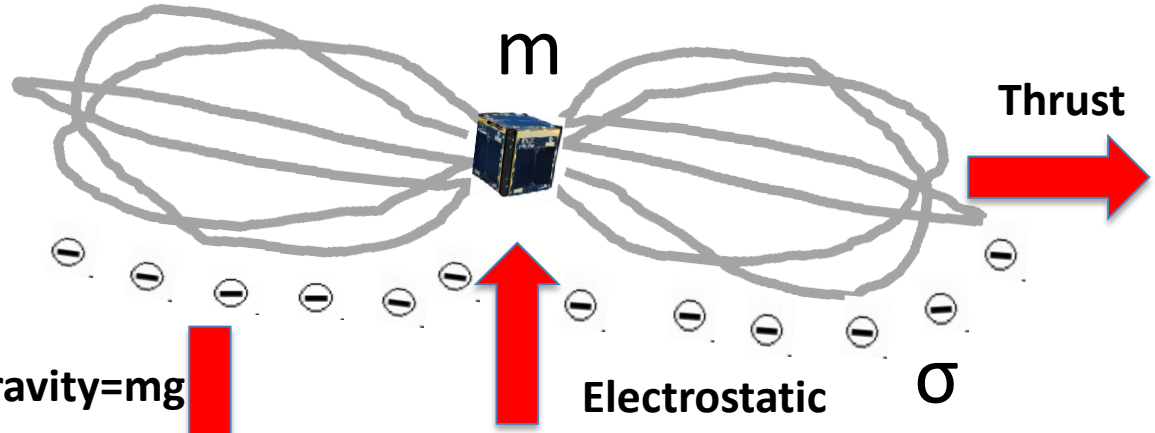

Electric field due to surface charge distribution σ:
$E = \sigma/(4\pi\varepsilon_0)$

Charge density on disk of radius r:
$\sigma = q/S = q/(\pi R^2) \rightarrow$
$q = 4\pi^2\varepsilon_0\pi R^2 E$

Issues:
- *Debye length*
- *How much charge available?*

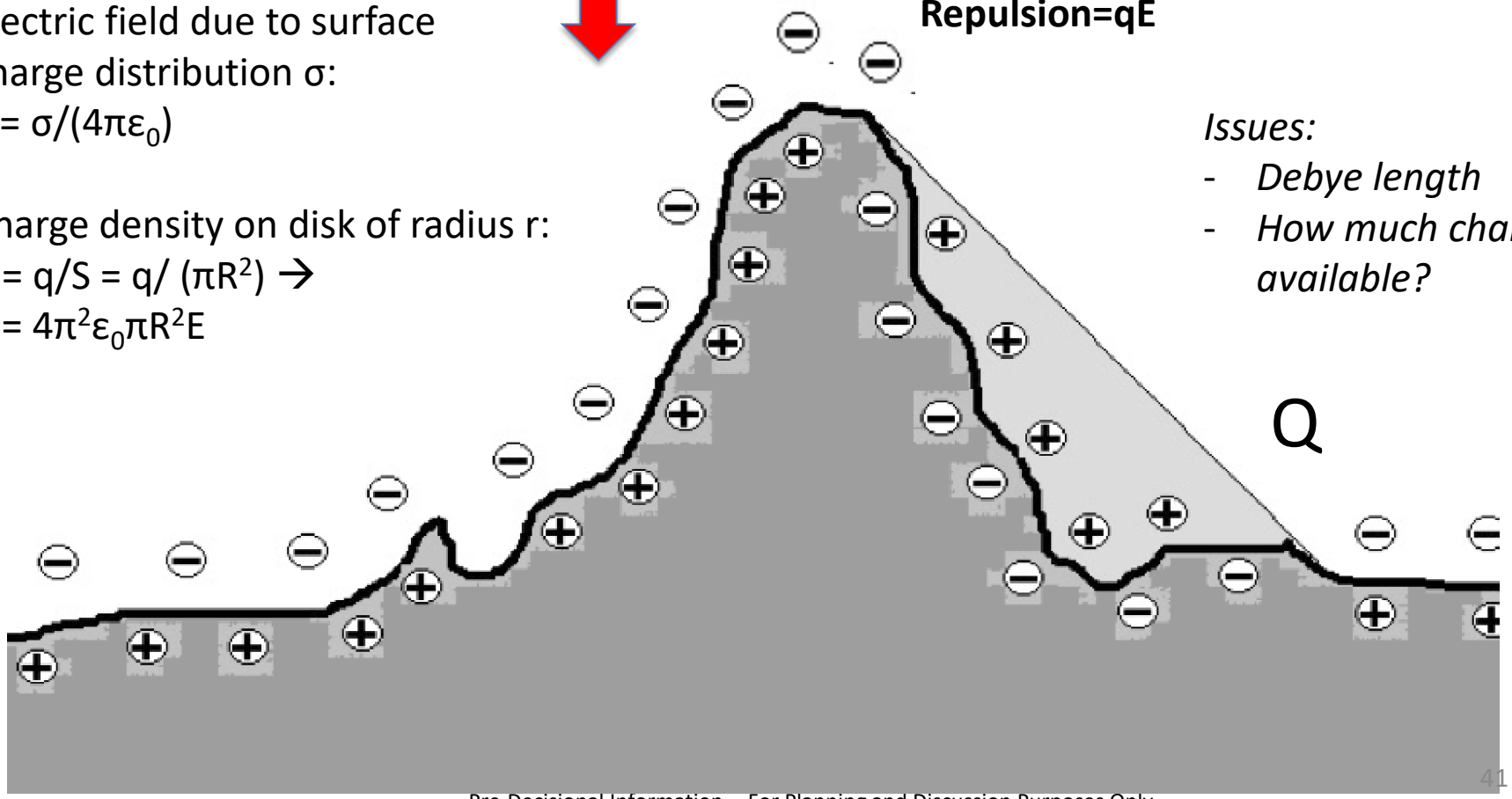

Pre-Decisional Information -- For Planning and Discussion Purposes Only
© 2016 California Institute of Technology. Government sponsorship acknowledged.

marco.b.quadrelli@jpl.nasa.gov

E-Glider equilibrium

- [Aplin] shows that electric fields of E~100-300 kV/m could take place on Itokawa, and an electric field of E=-10 V/m has been measured on the surface of the Moon under full Sun's illumination, therefore a wide range of E is to be considered.

- Assuming a gravity acceleration level of $g=10^{-5}$ m/s^2, typical of asteroids such as Itokawa, and denoting by R the equivalent radius of the levitated object, the dynamical equilibrium between gravity and electrostatic shows that the mass that can be levitated can be expressed as

$$m=4\pi\varepsilon_0 R^2 E^2/g$$

where ε_0 is the permittivity of vacuum:

- with 10 V, a 1 kg payload (point A, like a Cubesat, not including mass of wings) could be levitated with wings 200 m radius,
- a 500 kg payload (point B, like the Rosetta spacecraft) could be levitated with wings of 10 m radius if the field was close to 1 kV.

Pre-Decisional Information -- For Planning and Discussion Purposes Only
© 2016 California Institute of Technology. Government sponsorship acknowledged.

marco.b.quadrelli@jpl.nasa.gov

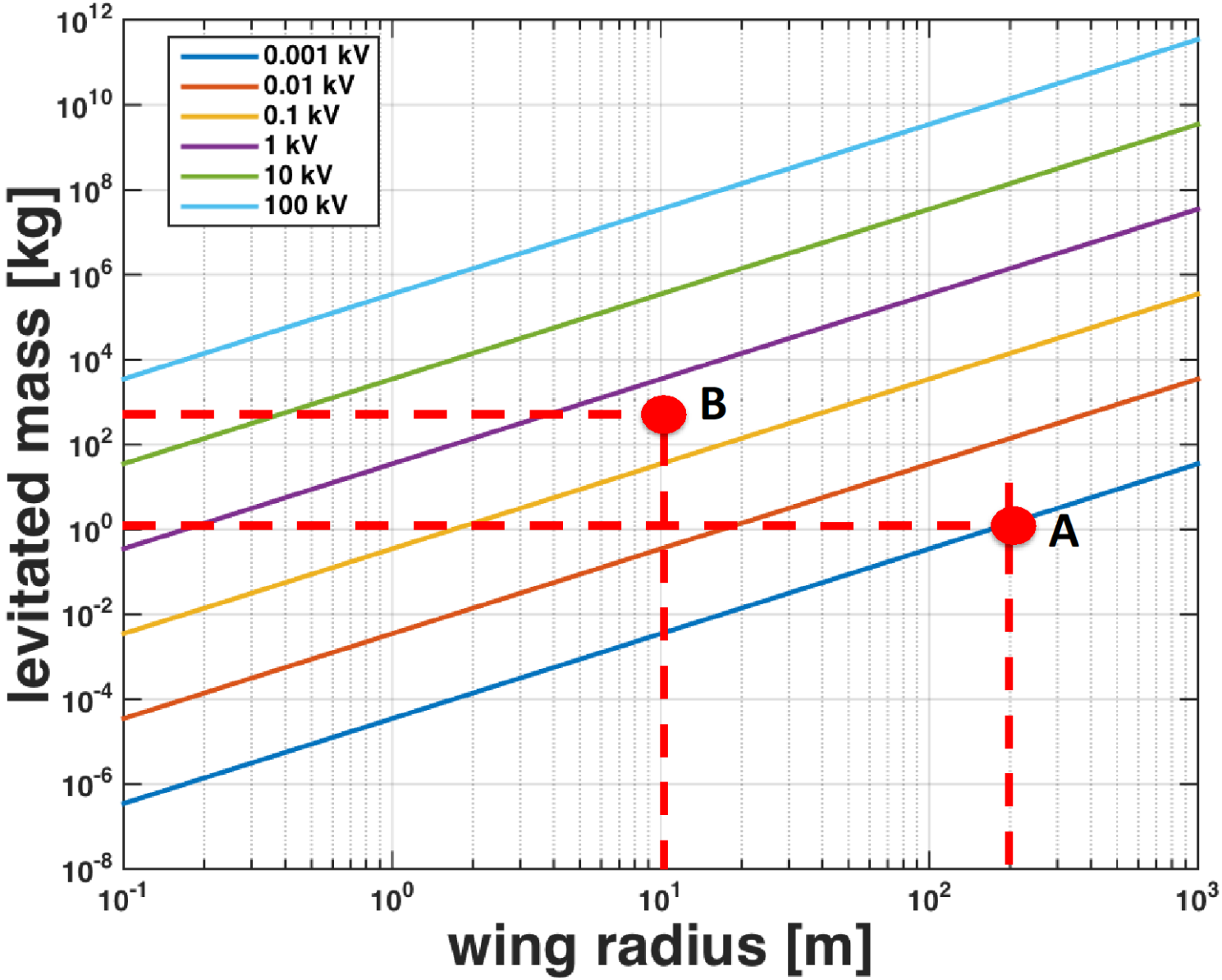

Pre-Decisional Information -- For Planning and Discussion Purposes Only
© 2016 California Institute of Technology. Government sponsorship acknowledged.

marco.b.quadrelli@jpl.nasa.gov

Challenges

- *Vehicle will become electrically neutral and unable to levitate*
  - *Use electron emitters on top side, while bottom side have opposite charge to surface*
- *Too much uncertainty in dust density and electrostatic potential distribution*
  - *We will map it during the reconnaissance phase. Will measure charge around vehicle during flight.*
- *How much fuel (RCS) is required for take-off/landing?*
  - *Will look at reference lift-off/flight/landing trajectory in relevant environment and do analysis assessment in simulation*
- *Can we actually lift 10 kg electrostatically? Where would the extra power come from?*
  - *Will still have battery (fuel cell) and solar panels, plus unused charge difference could be stored*

Pre-Decisional Information -- For Planning and Discussion Purposes Only
© 2016 California Institute of Technology. Government sponsorship acknowledged.
marco.b.quadrelli@jpl.nasa.gov

Mechanics of Electrostatic Inflation

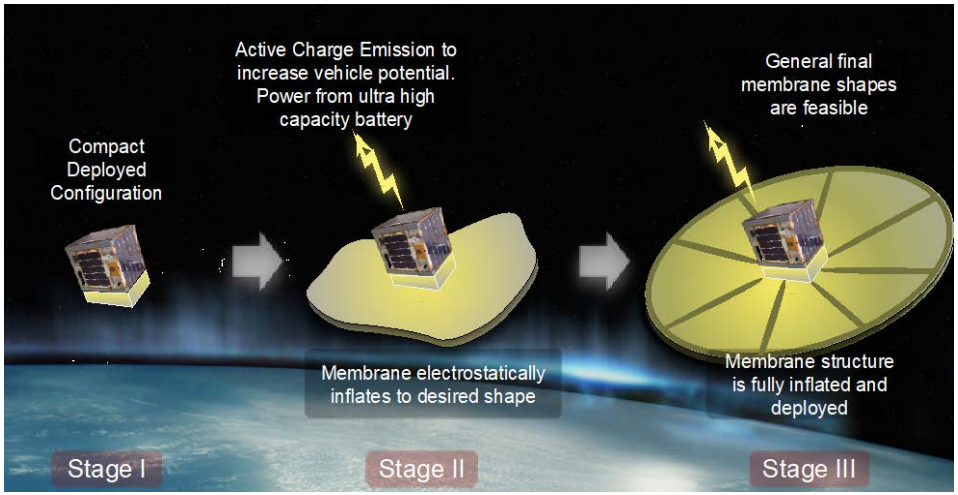

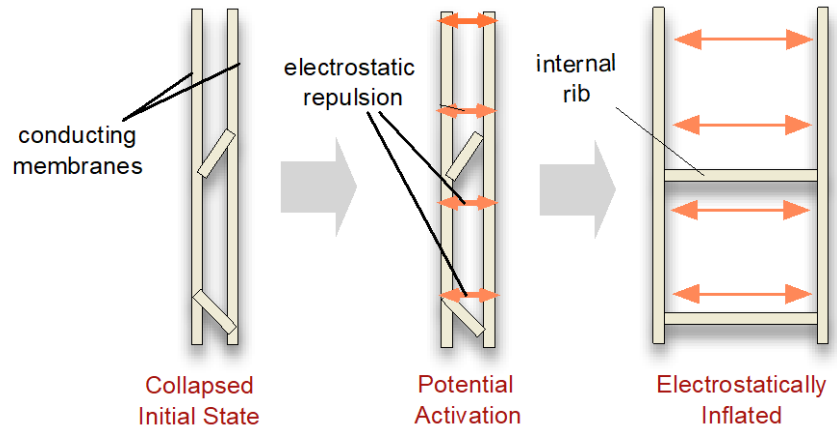

Minimum required surface charge density for electrostatic Inflation at GEO and LEO for a range of plate areas

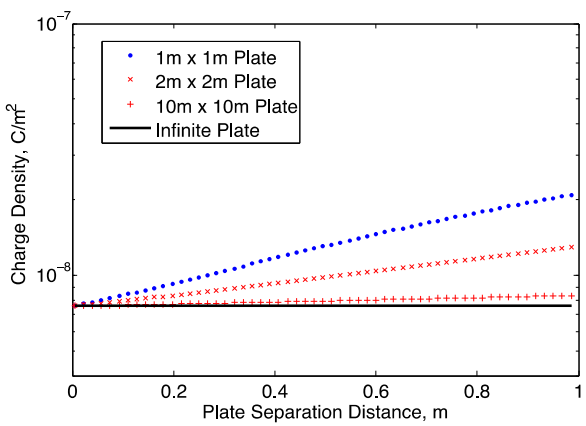

a) GEO Along Track Configuration

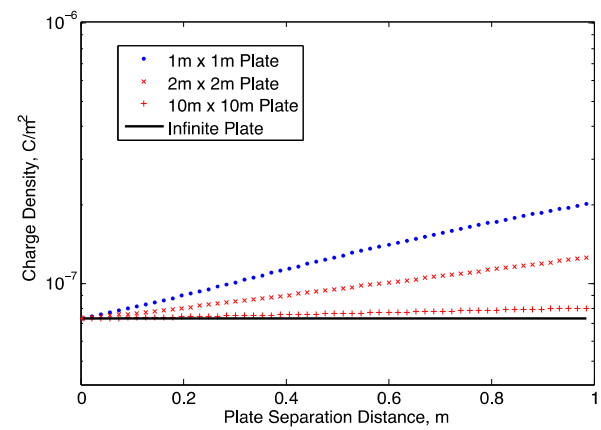

b) LEO Along Track Configuration, 300 km altitude

Courtesy of Hanspeter Schaub, UC Boulder

Pre-Decisional Information -- For Planning and Discussion Purposes Only
© 2016 California Institute of Technology. Government sponsorship acknowledged.

marco.b.quadrelli@jpl.nasa.gov

Electrostatic Inflation Experiments

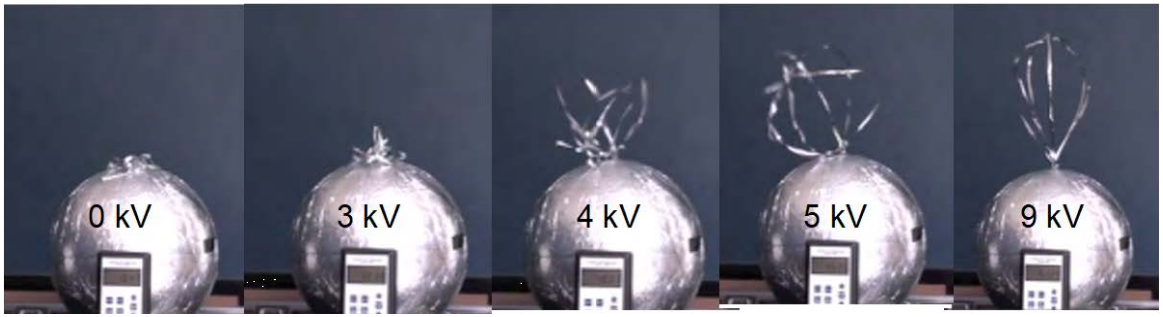

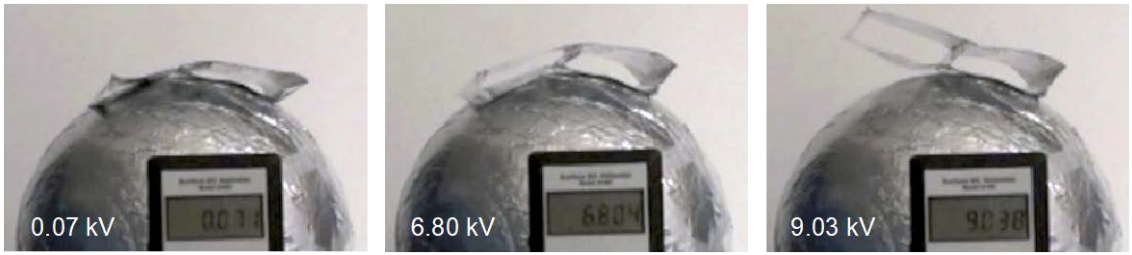

The wings could be made of very thin charged Mylar film, or long charged Mylar strands, which as in the Earth's Gossamer spider, are electrostatically inflated, as demonstrated in Figure 3a taken from [Stiles2010, Stiles2011, Stiles2012], and would provide the lift due to electrostatic repulsion.

Further articulation at the root of the lateral strands or inflated membrane wings, would generate a component of lift depending on the articulation angle, hence a selective maneuvering capability which, to all effects, would lead to electrostatic (rather than aerodynamic) flight.

Courtesy of Hanspeter Schaub, UC Boulder

Pre-Decisional Information -- For Planning and Discussion Purposes Only
© 2016 California Institute of Technology. Government sponsorship acknowledged.

marco.b.quadrelli@jpl.nasa.gov

Phase II experiments in JPL Bell Jar

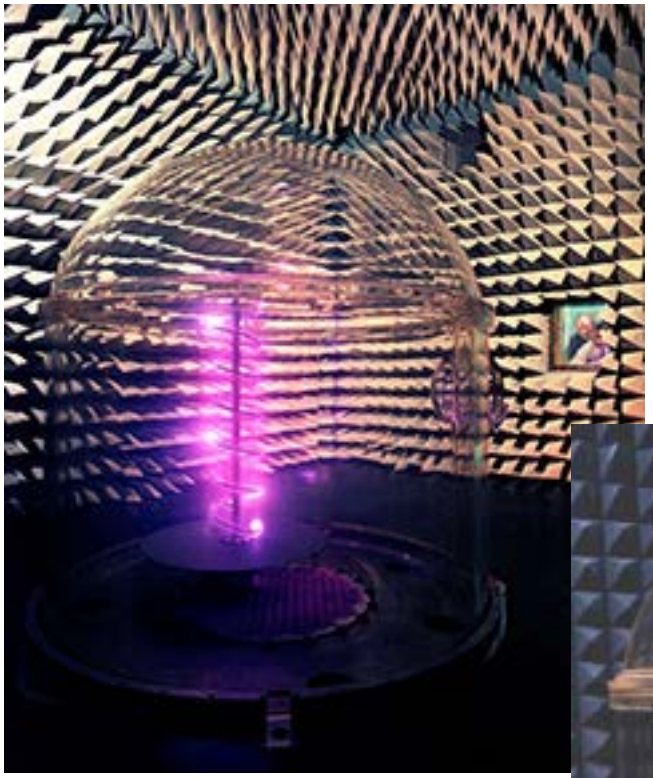

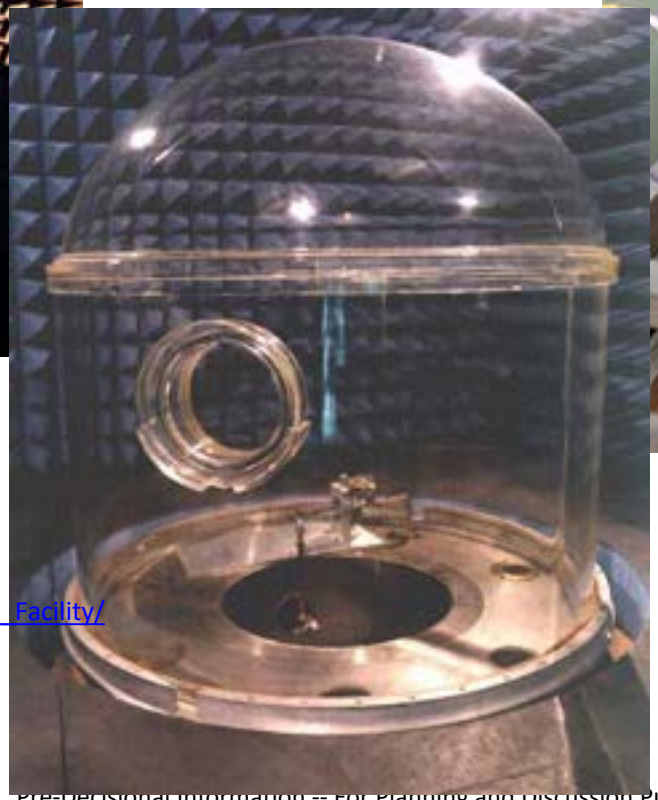

http://mesa.jpl.nasa.gov/Vaccuum_Breakdown_Facility/

Pre-Decisional Information -- For Planning and Discussion Purposes Only
© 2016 California Institute of Technology. Government sponsorship acknowledged.

marco.b.quadrelli@jpl.nasa.gov

E-Glider preliminary design

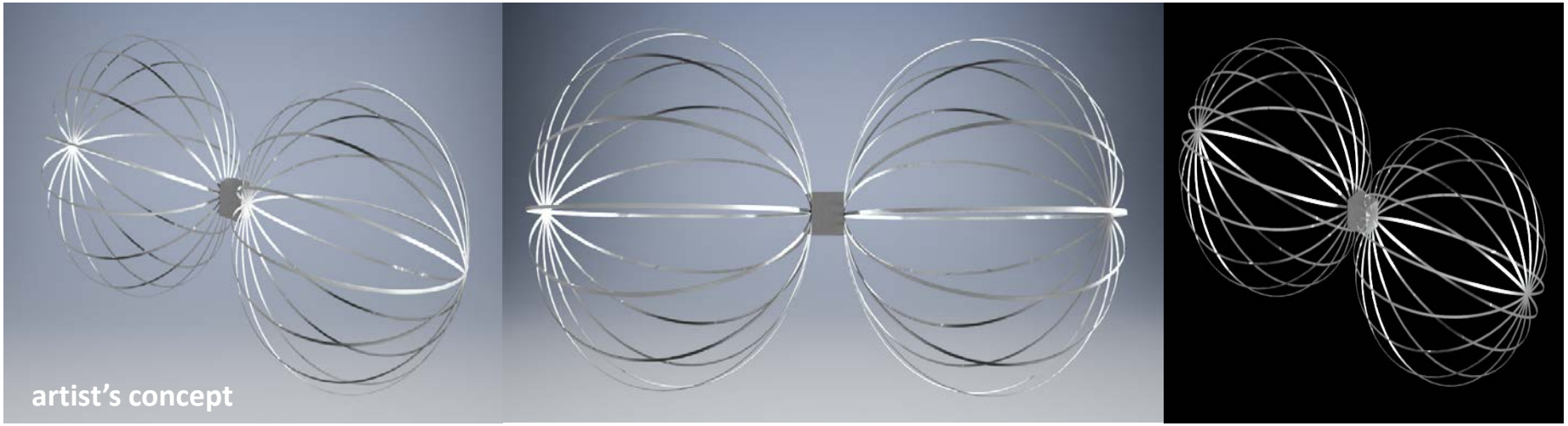

- Cube: .12x.12x.1 m (based on MINERVA)
- Ring diameter: 1 m

Pre-Decisional Information -- For Planning and Discussion Purposes Only
© 2016 California Institute of Technology. Government sponsorship acknowledged.

marco.b.quadrelli@jpl.nasa.gov

Animations

Pre-Decisional Information -- For Planning and Discussion Purposes Only
© 2016 California Institute of Technology. Government sponsorship acknowledged.

marco.b.quadrelli@jpl.nasa.gov

E-Glider at Itokawa

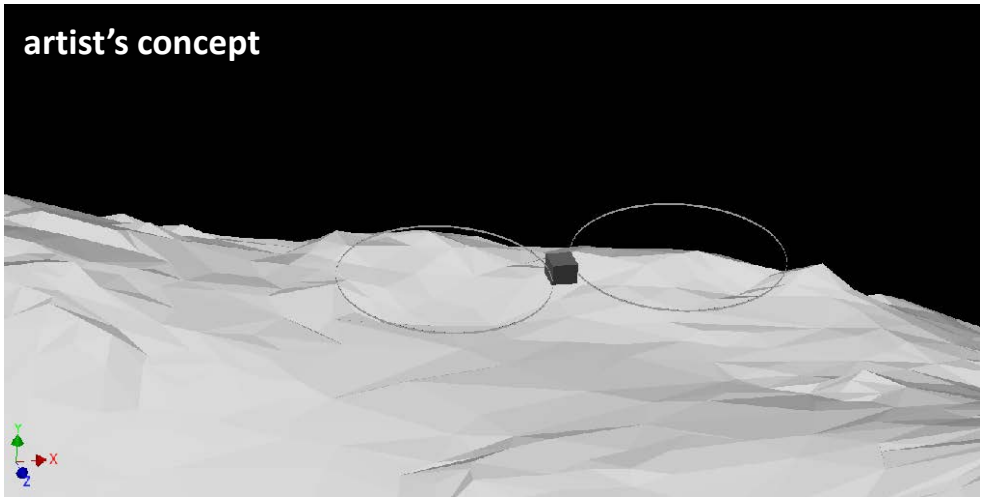

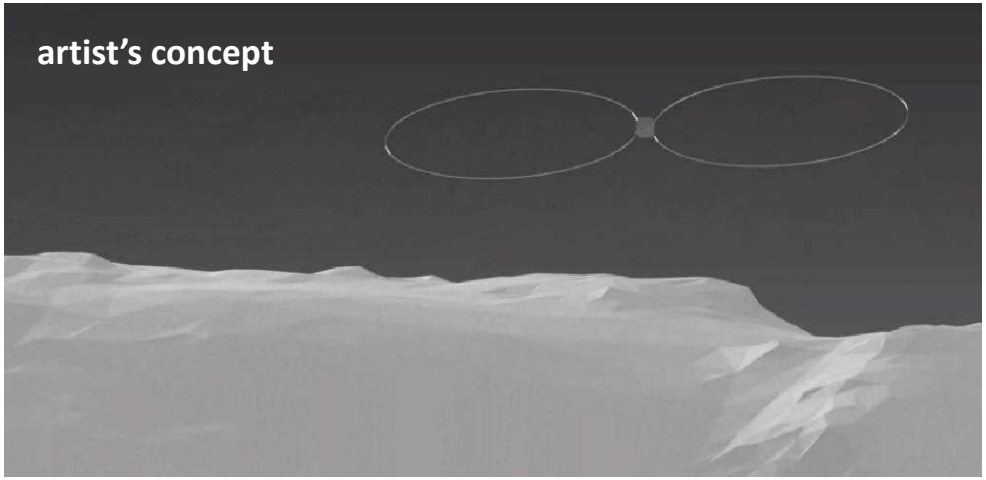

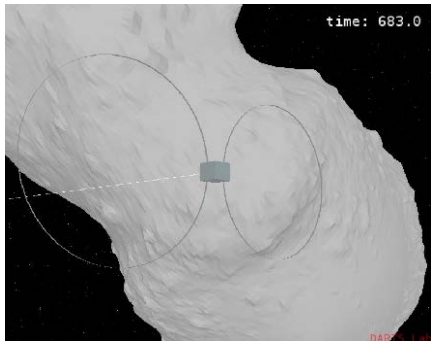

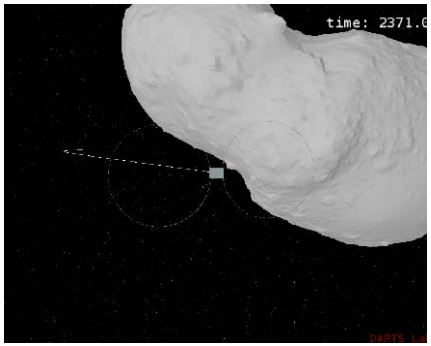

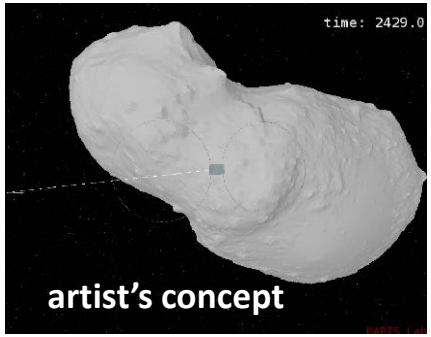

Pre-Decisional Information -- For Planning and Discussion Purposes Only
© 2016 California Institute of Technology. Government sponsorship acknowledged.

marco.b.quadrelli@jpl.nasa.gov

Orbital dynamics model

- Equation of motion: Cowell's formulation $\ddot{\vec{r}} = -\frac{\mu}{r^3}\vec{r} + \vec{a}_{perturbed}$
- Perturbing effects added as additional terms: central body asphericity and solar radiation pressure
- Total gravitational pull is due to: Potential of a sphere + Asphericity potential. Asphericity potential derived from spherical-harmonic expansion

$$U = \frac{\mu}{r}(1 + \sum_{l=2}^{\infty}\sum_{m=0}^{l}(\frac{r_0}{r})^l P_{lm}[\sin(\phi_{sat})](C_{lm}\cos(m\lambda_{sat}) + S_{lm}\sin(m\lambda_{sat})))$$

- C(l,m) and S(l,m) represent the mathematical modeling of Itokawa's shape. Computing the gradient of **U** we can obtain the three components of the acceleration
- Incident radiation produces two forces, the first one is due to absorbed photons, the second due to reflected photons. We assume the spacecraft to be always perpendicular to the sun-line and at a constant distance **d**. **ρ** is the reflectivity coefficient, **P0** is a constant relative to the sun and **Bsc** is the spacecraft mass to exposed area ratio

$$\vec{a} = -\frac{(1+\rho)P_0}{B_{SC}d^3}\vec{d}$$

Pre-Decisional Information -- For Planning and Discussion Purposes Only
© 2016 California Institute of Technology. Government sponsorship acknowledged.
marco.b.quadrelli@jpl.nasa.gov

Orbiting Itokawa

Parameter	Symbol	Value	Units
Universal gravitational constant	G	$6.7 \cdot 10^{-11}$	$m^3 kg^{-1} s^{-2}$
Itokawa Semi-Major Axis	E	1.324	AU
Gravitational Parameter	μ	$2.36 \cdot 10^{-9}$	$km^3 s^{-2}$
Rotation Period	T_r	12.132	hours
Mean Radius	r_0	0.162	km

Order l	Degree m	C Coefficient C_{lm}	S Coefficient S_{lm}
0	0	1.0	-
1	0	0.0	-
1	1	0.0	0.0
2	0	−0.145216	-
2	1	0.0	0.0
2	2	0.219420	0.0
3	0	0.036115	-
3	1	−0.028139	−0.006137
3	2	−0.046894	−0.046894
3	3	0.069022	0.033976
4	0	0.087852	-
4	1	0.034069	0.004870
4	2	−0.123263	0.000098
4	3	−0.030673	−0.015026
4	4	0.150282	0.011627

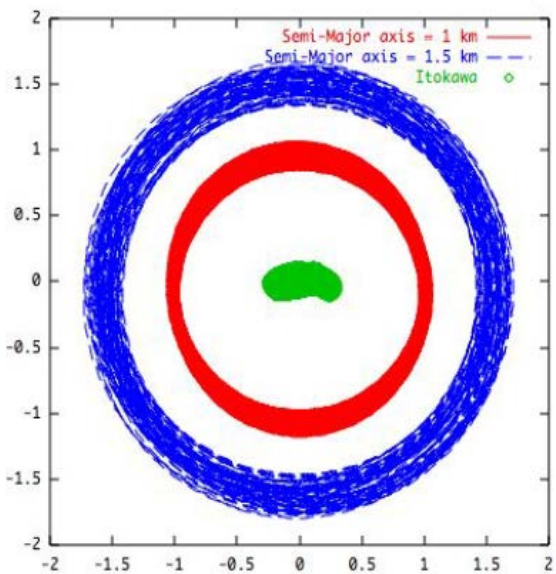

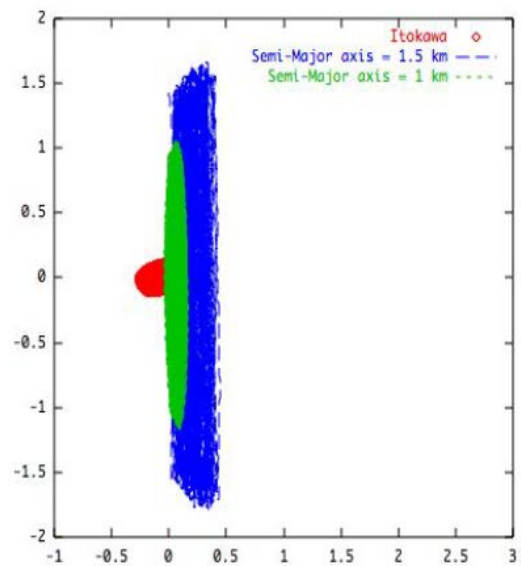

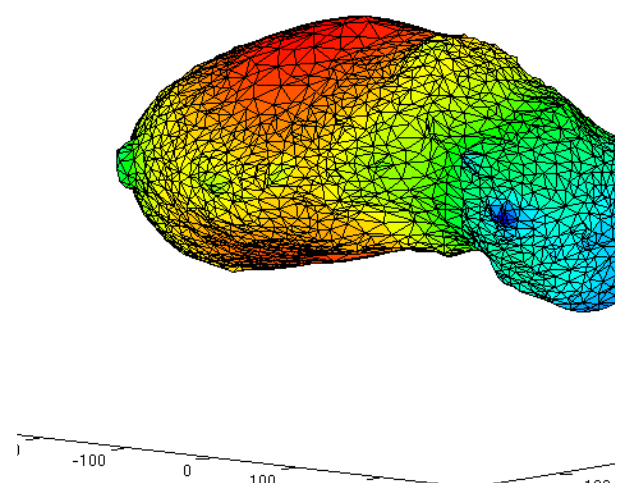

Pre-Decisional Information -- For Planning and Discussion Purposes Only
© 2016 California Institute of Technology. Government sponsorship acknowledged.

marco.b.quadrelli@jpl.nasa.gov

Force Analysis Parameters

Assumptions

1. The body (Earth or Itokawa) are modeled as point charge and masses (spherical gravity and spherical distribution of charge)
2. The charge of the body is (currently) set to be equal and opposite the charge of the particle, rod, and hoop
3. The hoop is aligned so that it is normal to the body
4. All of the forces were calculated in Matlab based on potentials from MacMillan

Common Values

- For these plots, the particle, rod, and hoop are all positioned 2 m above the surface of the body
- Radius of Earth: 6371 km (1)
- Mass of Earth: $5.972*10^{24}$ kg (1)
- Mass of Itokawa: $3.51*10^{10}$ kg (2)
- (Average) Radius of Itokawa: 191.94 m
  - found by taking the average magnitude of the surface vectors from the DARTS lab Itokawa data file. Average Itokawa radius agrees with the dimension values reported in (1)
- Density of particle, rod, and hoop: 1400 kg/m^3 (3).

Pre-Decisional Information -- For Planning and Discussion Purposes Only
© 2016 California Institute of Technology. Government sponsorship acknowledged.
marco.b.quadrelli@jpl.nasa.gov

Potential from a Particle

- To approximate a particle, the length and diameter of the rod were taken to be much smaller than the distance to the test point
- In this configuration, a 2 mm long, 2 mm diameter particle has an equilibrium charge of ~ 14 mC

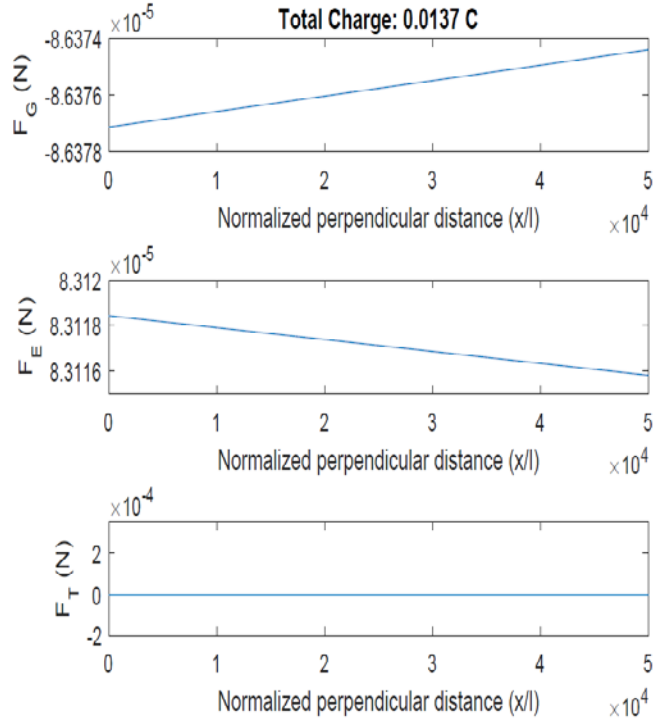

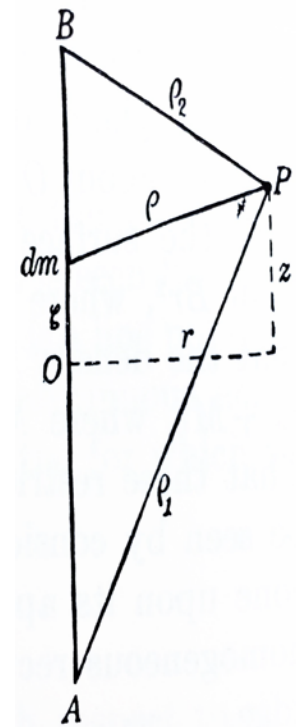

$$V = \sigma log \frac{\rho_1 + \rho_2 + 2l}{\rho_1 + \rho_2 - 2l}$$

$$F_x = \frac{\partial V}{\partial x} = -\frac{2lx\left(\frac{1}{\sqrt{(l+z)^2+x^2}} + \frac{1}{\sqrt{(l-z)^2+x^2}}\right)}{-l^2 + \sqrt{(l-z)^2+x^2}\sqrt{(l+z)^2+x^2} + x^2 + z^2}$$

William Duncan MacMillan. The theory of the potential. Dover, 1958.

Pre-Decisional Information -- For Planning and Discussion Purposes Only
© 2016 California Institute of Technology. Government sponsorship acknowledged.

marco.b.quadrelli@jpl.nasa.gov

Total force for particle

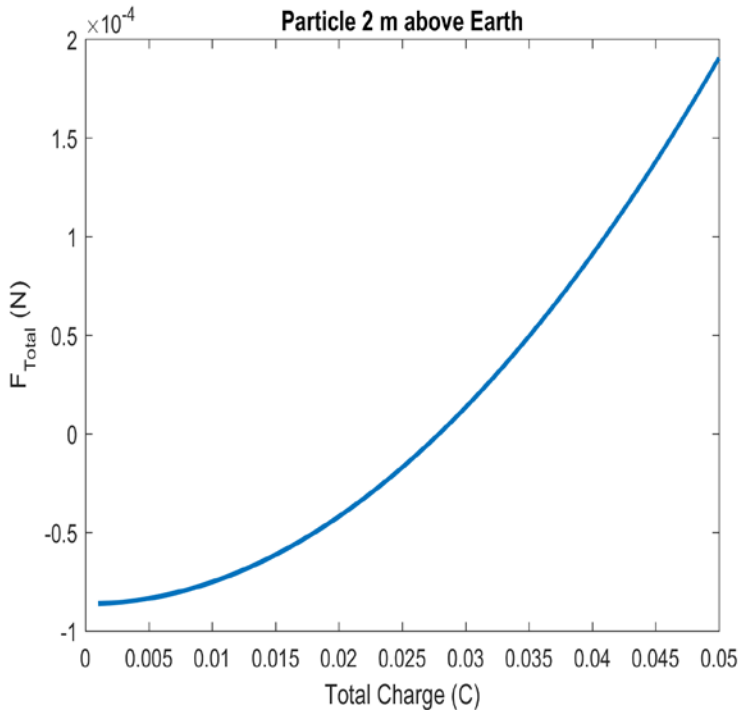

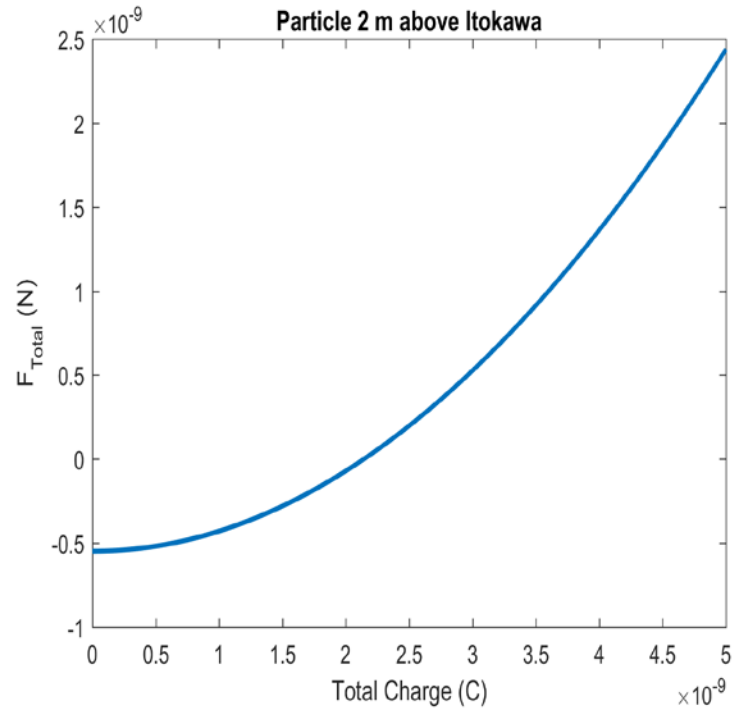

The radius of the particle is 1 mm and the length is 2 mm.

Pre-Decisional Information -- For Planning and Discussion Purposes Only
© 2016 California Institute of Technology. Government sponsorship acknowledged.

marco.b.quadrelli@jpl.nasa.gov

Potential from a Straight Rod

- The electrostatic and gravitational forces for a straight rod evaluated at a point were calculated by taking the derivative of the potential given by MacMillan and multiplying by the appropriate coefficients
- For a 2 m long, 1 cm diameter Mylar rod, the electrostatic force was strong enough to oppose the Earth's gravitational force when the rod had ~70 C of charge

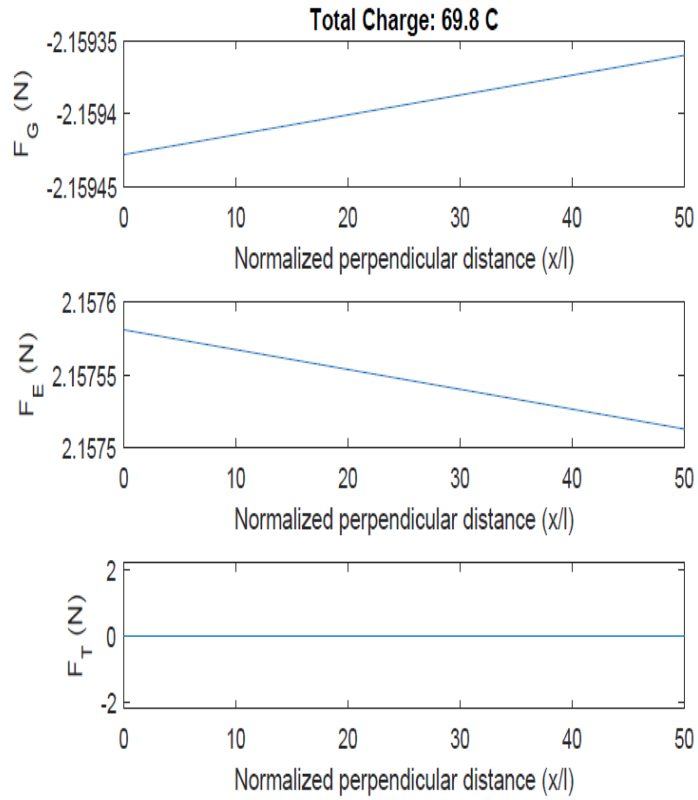

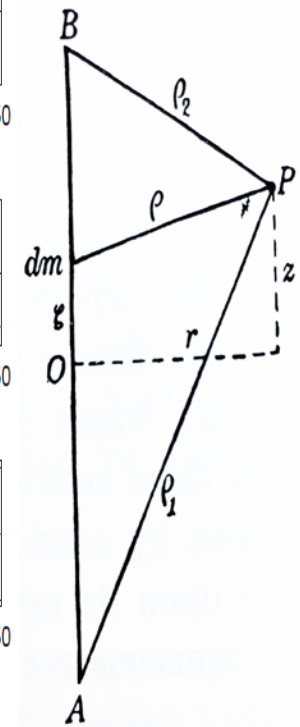

$$V = \sigma log \frac{\rho_1 + \rho_2 + 2l}{\rho_1 + \rho_2 - 2l}$$

$$F_x = \frac{\partial V}{\partial x} = -\frac{2lx\left(\frac{1}{\sqrt{(l+z)^2+x^2}} + \frac{1}{\sqrt{(l-z)^2+x^2}}\right)}{-l^2 + \sqrt{(l-z)^2+x^2}\sqrt{(l+z)^2+x^2} + x^2 + z^2}$$

William Duncan MacMillan. The theory of the potential. Dover, 1958.

Pre-Decisional Information -- For Planning and Discussion Purposes Only
© 2016 California Institute of Technology. Government sponsorship acknowledged.

marco.b.quadrelli@jpl.nasa.gov

Total force for rod

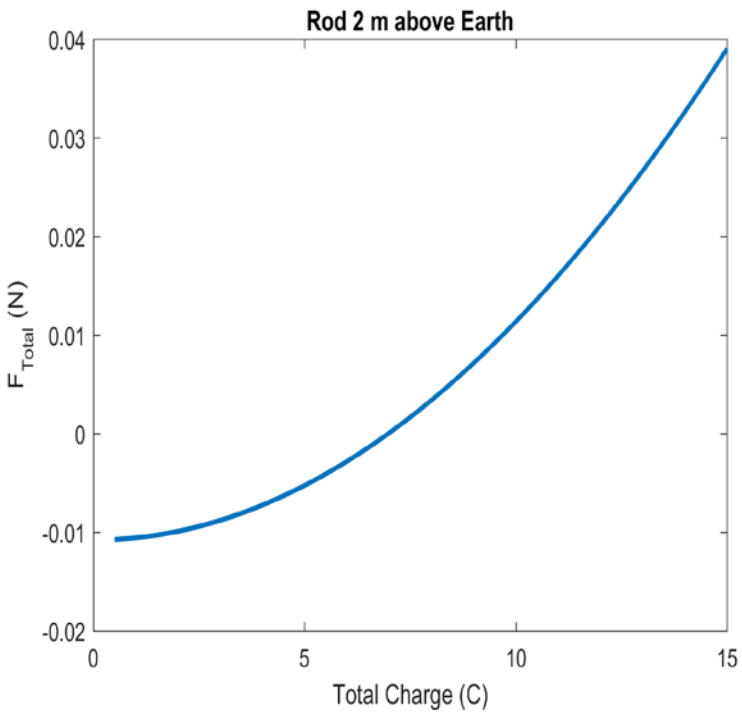

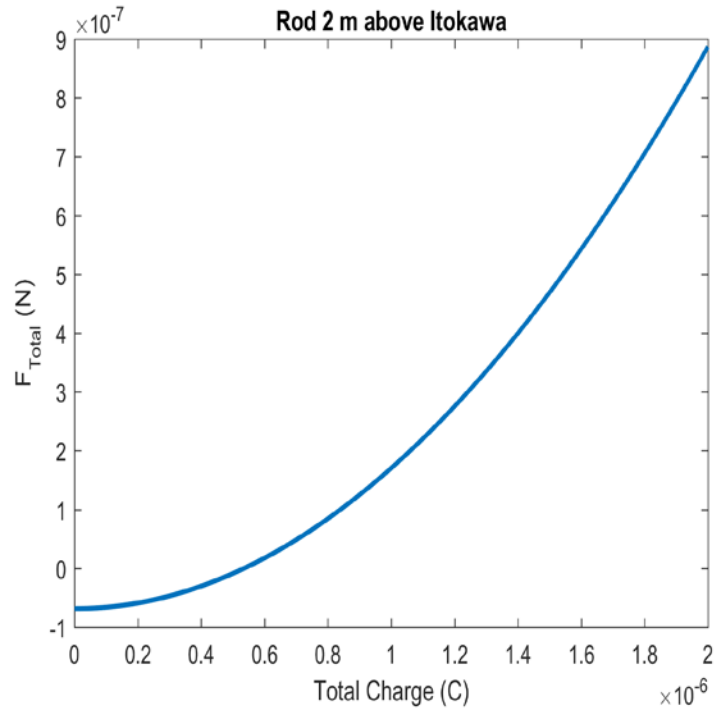

The radius of the rod is 0.5 mm and the length is 1 m.

Pre-Decisional Information -- For Planning and Discussion Purposes Only
© 2016 California Institute of Technology. Government sponsorship acknowledged.

marco.b.quadrelli@jpl.nasa.gov

Potential from a Hoop

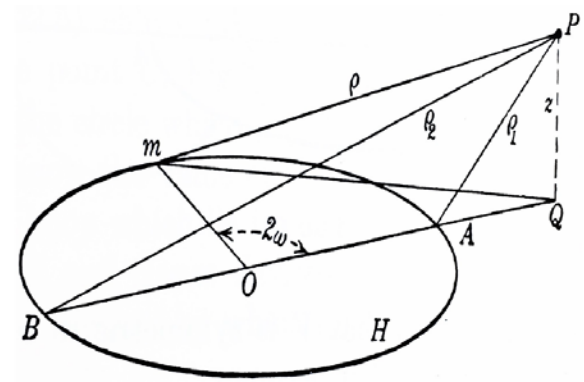

- Similarly, the equilibrium charge on a thin Mylar hoop was calculated following the derivation in MacMillan
- V is the potential for any orientation of the hoop, which simplifies to V_a when the plane of the hoop is normal to the test point and ρ_a is the common length between each edge to the point
- For a 1 cm tall, 1 m diameter, 500 µm thick hoop, the equilibrium charge is ~ 22 mC

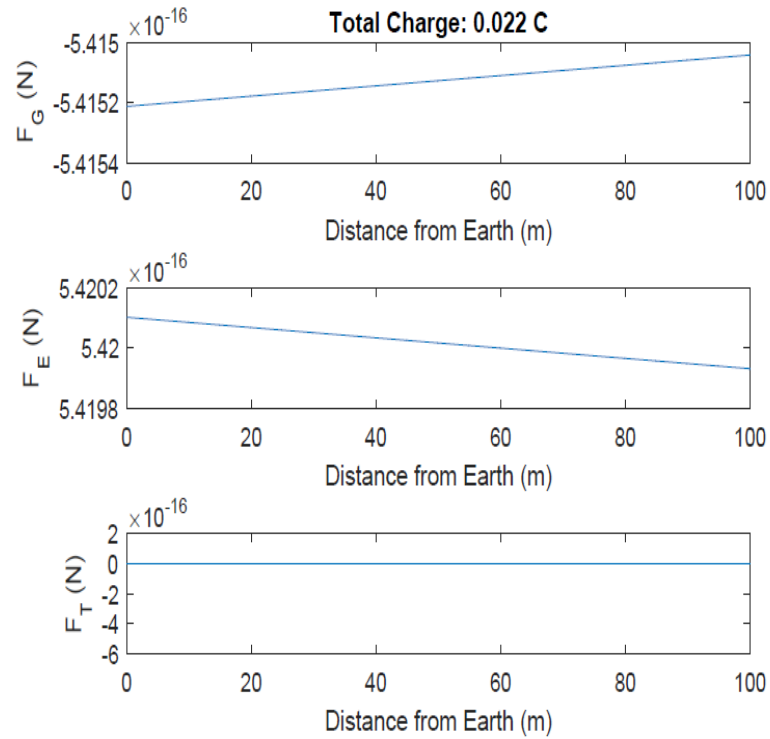

William Duncan MacMillan. The theory of the potential. Dover, 1958.

$$V = \frac{2M}{\pi}\int_0^{\frac{\pi}{2}} \frac{d\omega}{\sqrt{\rho_1^2 cos^2\omega + \rho_2^2 sin^2\omega}} \qquad V_a = \frac{M}{\rho_a} \qquad F = -\frac{M}{\rho_a^2}$$

Pre-Decisional Information -- For Planning and Discussion Purposes Only
© 2016 California Institute of Technology. Government sponsorship acknowledged.

marco.b.quadrelli@jpl.nasa.gov

Total force for hoop

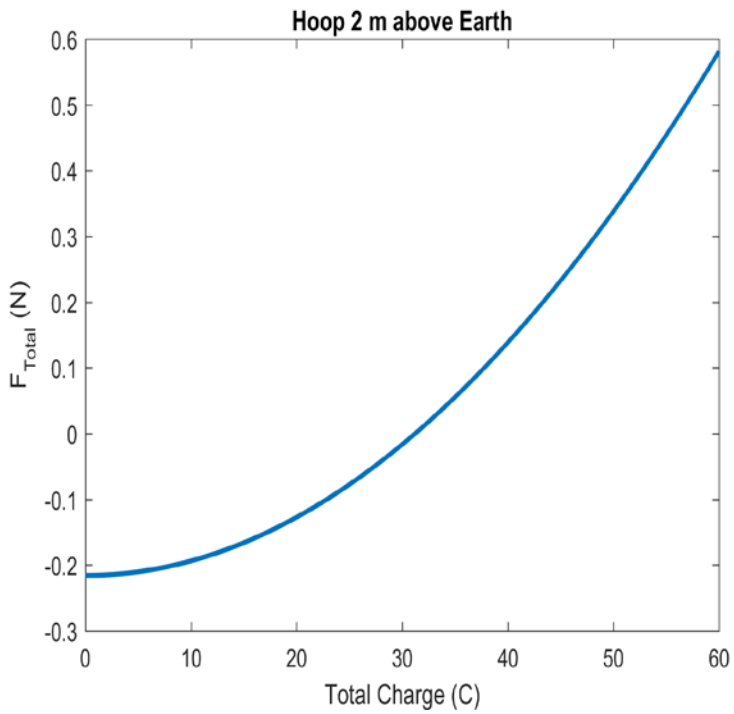

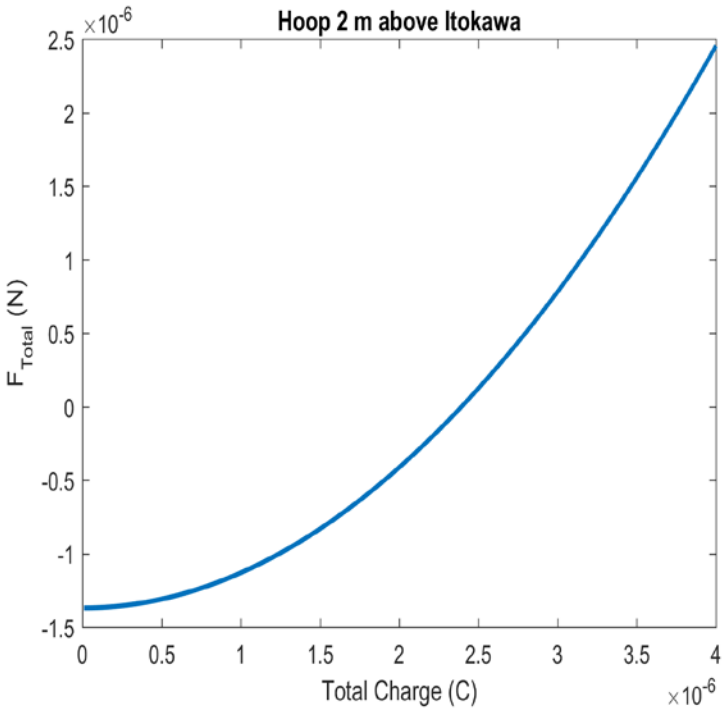

The outer radius of the hoop is 0.5 m, the thickness is 0.5 mm, and the height is 1 cm.

Pre-Decisional Information -- For Planning and Discussion Purposes Only
© 2016 California Institute of Technology. Government sponsorship acknowledged.

marco.b.quadrelli@jpl.nasa.gov

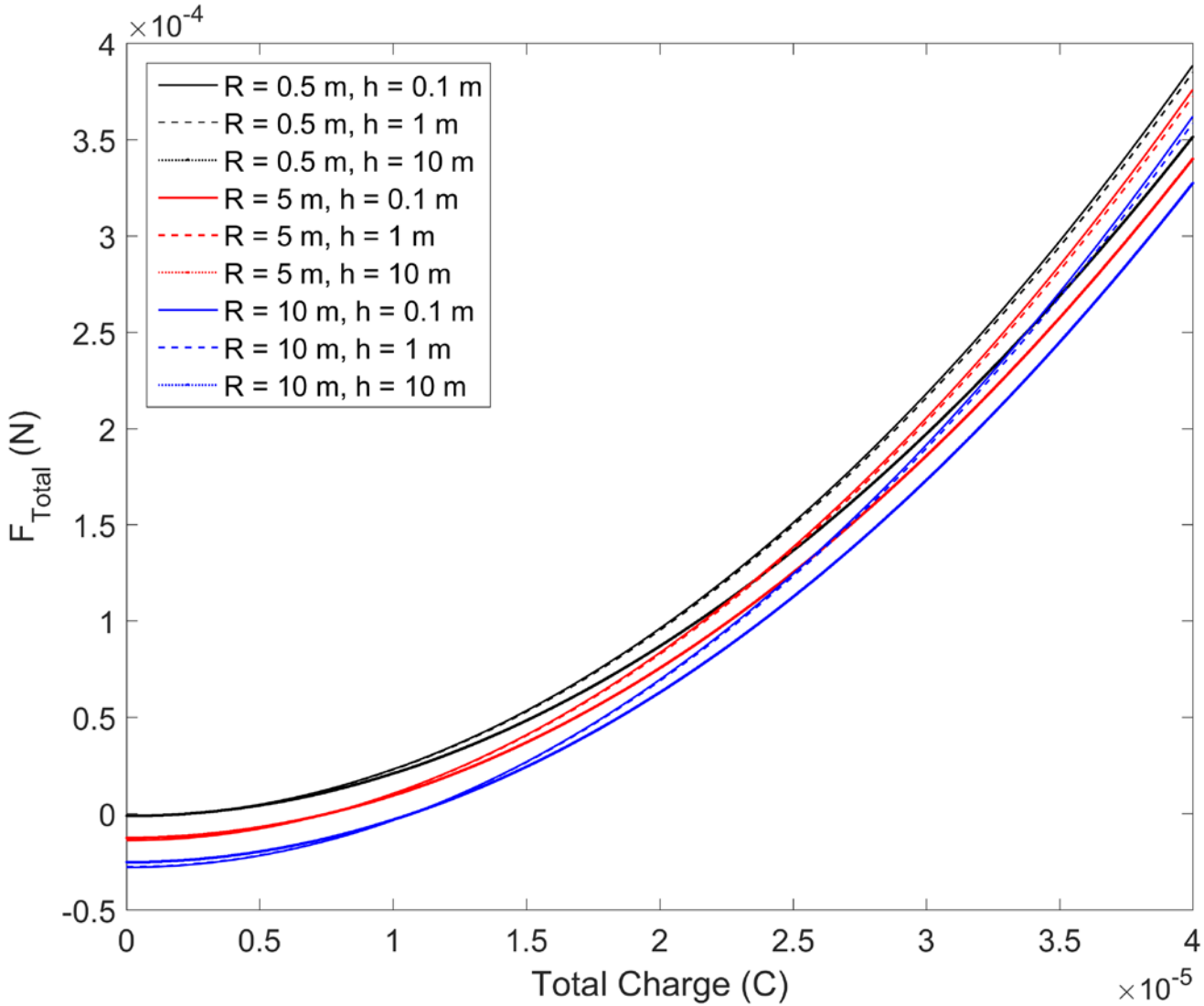

Pre-Decisional Information -- For Planning and Discussion Purposes Only
© 2016 California Institute of Technology. Government sponsorship acknowledged.

marco.b.quadrelli@jpl.nasa.gov

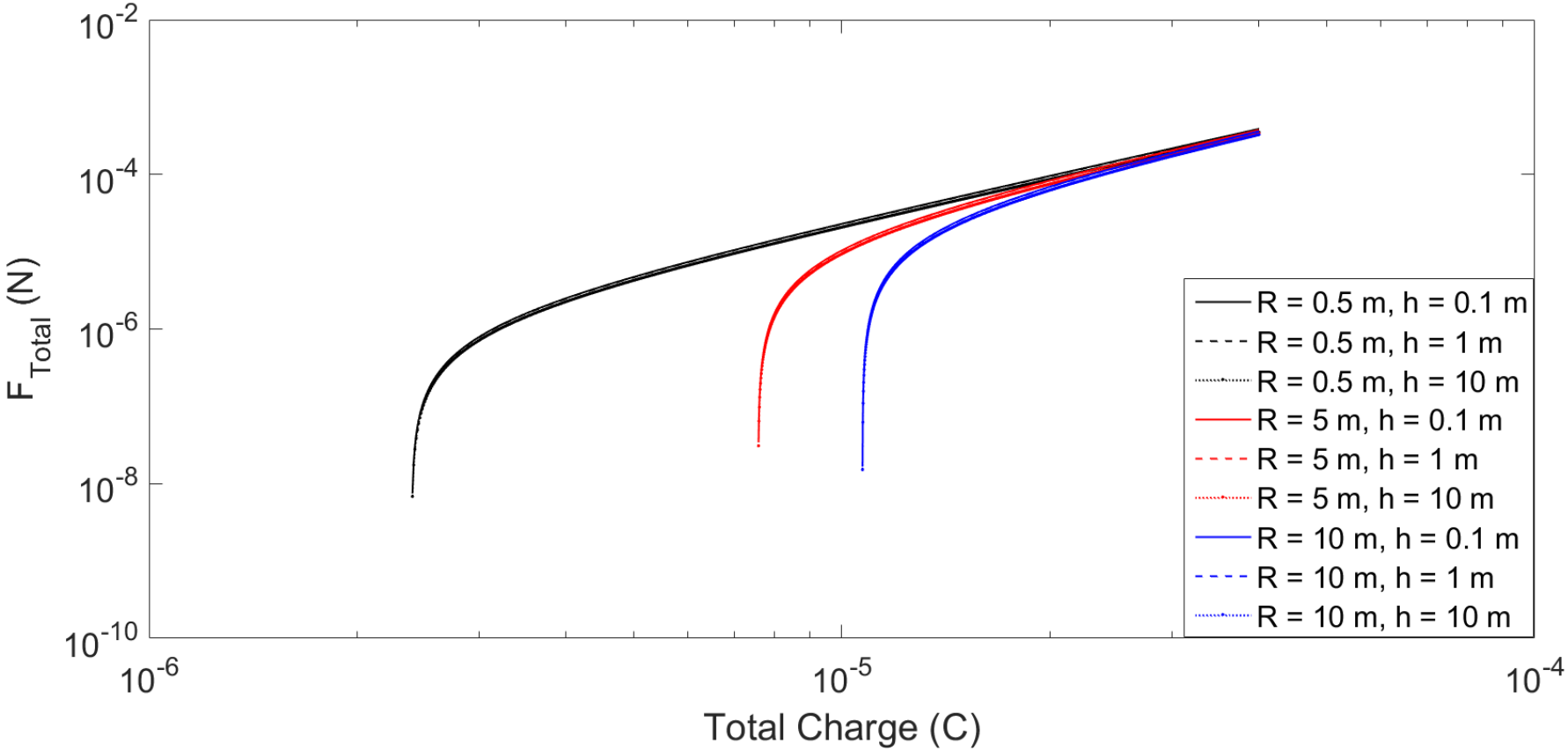

Pre-Decisional Information -- For Planning and Discussion Purposes Only
© 2016 California Institute of Technology. Government sponsorship acknowledged.

marco.b.quadrelli@jpl.nasa.gov

Interaction potential for extended body

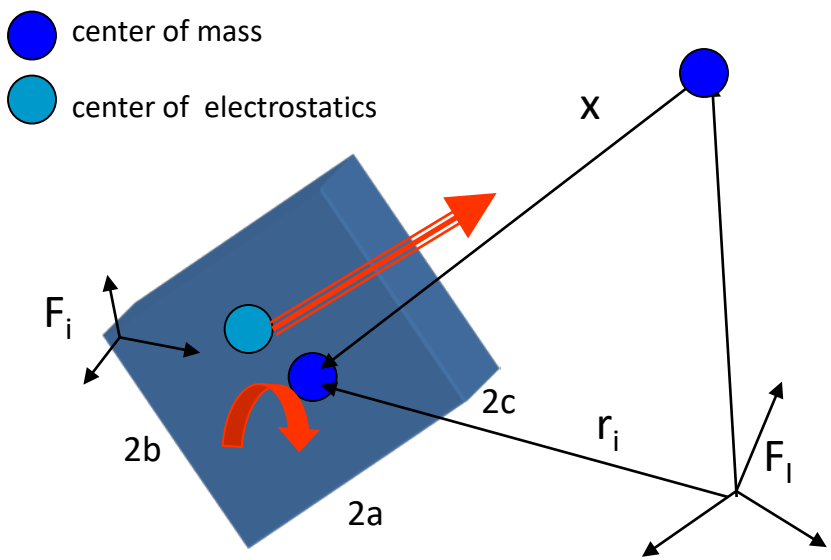

The interaction between extended bodies results in a force and a torque

→ By morphing the E-Glider wings we obtain both longitudinal and lateral displacements

```
Vaa(1)  =+(x1+a)*(x2+b)*log((r1+r2+2*c)/(r1+r2-2*c));
Vaa(2)  =-(x1+a)*(x2-b)*log((r3+r4+2*c)/(r3+r4-2*c));
Vaa(3)  =+(x1+a)*(x3+c)*log((r1+r3+2*b)/(r1+r3-2*b));
Vaa(4)  =-(x1+a)*(x3-c)*log((r2+r4+2*b)/(r2+r4-2*b));
Vaa(5)  =+(x1-a)*(x2-b)*log((r7+r8+2*c)/(r7+r8-2*c));
Vaa(6)  =-(x1-a)*(x2+b)*log((r5+r6+2*c)/(r5+r6-2*c));
Vaa(7)  =+(x1-a)*(x3-c)*log((r6+r8+2*b)/(r6+r8-2*b));
Vaa(8)  =-(x1-a)*(x3+c)*log((r5+r7+2*b)/(r5+r7-2*b));
Vaa(9)  =+(x2+b)*(x3+c)*log((r1+r5+2*a)/(r1+r5-2*a));
Vaa(10)=-(x2+b)*(x3-c)*log((r2+r6+2*a)/(r2+r6-2*a));
Vaa(11)=+(x2-b)*(x3-c)*log((r4+r8+2*a)/(r4+r8-2*a));
Vaa(12)=-(x2-b)*(x3+c)*log((r3+r7+2*a)/(r3+r7-2*a));
Va=sum(Vaa);
```

Potential V=Va+Vb

```
Vbb(1)=atan((x2+b)*(x3-c)/((x1+a)*r2))-...
       atan((x2+b)*(x3+c)/((x1+a)*r1))+...
       atan((x2-b)*(x3+c)/((x1+a)*r3))-...
       atan((x2-b)*(x3-c)/((x1+a)*r4));
Vbb(2)=atan((x2+b)*(x3+c)/((x1-a)*r5))-...
       atan((x2+b)*(x3-c)/((x1-a)*r6))+...
       atan((x2-b)*(x3-c)/((x1-a)*r8))-...
       atan((x2-b)*(x3+c)/((x1-a)*r7));
Vbb(3)=atan((x1-a)*(x3+c)/((x2+b)*r5))-...
       atan((x1+a)*(x3+c)/((x2+b)*r1))+...
       atan((x1+a)*(x3-c)/((x2+b)*r2))-...
       atan((x1-a)*(x3-c)/((x2+b)*r6));
Vbb(4)=atan((x1+a)*(x3+c)/((x2-b)*r3))-...
       atan((x1-a)*(x3+c)/((x2-b)*r7))+...
       atan((x1-a)*(x3-c)/((x2-b)*r8))-...
       atan((x1+a)*(x3-c)/((x2-b)*r4));
Vbb(5)=atan((x1+a)*(x2-b)/((x3+c)*r3))-...
       atan((x1+a)*(x2+b)/((x3+c)*r1))+...
       atan((x1-a)*(x2+b)/((x3+c)*r5))-...
       atan((x1-a)*(x2-b)/((x3+c)*r7));
Vbb(6)=atan((x1+a)*(x2+b)/((x3-c)*r2))-...
       atan((x1+a)*(x2-b)/((x3-c)*r4))+...
       atan((x1-a)*(x2-b)/((x3-c)*r8))-...
       atan((x1-a)*(x2+b)/((x3-c)*r6));
Vb=0.5*((x1+a)^2)*Vbb(1)+...
   0.5*((x1-a)^2)*Vbb(2)+...
   0.5*((x2+b)^2)*Vbb(3)+...
   0.5*((x2-b)^2)*Vbb(4)+...
   0.5*((x3+c)^2)*Vbb(5)+...
   0.5*((x3-c)^2)*Vbb(6);
```

$$\mathbf{F} = \frac{q_0}{4\pi\varepsilon_0 V_0}\left(\frac{\partial V_a}{\partial \mathbf{x}} + \frac{\partial V_b}{\partial \mathbf{x}}\right)$$

$$\mathbf{G} = \frac{q_0}{4\pi\varepsilon_0 V_0}\nabla_{\mathbf{x}} \otimes \left(\frac{\partial V_a}{\partial \mathbf{x}} + \frac{\partial V_b}{\partial \mathbf{x}}\right)$$

Pre-Decisional Information -- For Planning and Discussion Purposes Only
© 2016 California Institute of Technology. Government sponsorship acknowledged.

marco.b.quadrelli@jpl.nasa.gov

Summary of interaction model calculations

- The equilibrium forces for a particle, rod, and hoop were analyzed based on derivations from MacMillan
- As an initial exercise and to validate MacMillan's model, the forces of a very small rod (approximating a point charge) were calculated and found to be in excellent agreement with the general equation for point mass/charges in equilibrium
- The subsequent simulations provide a simplified analysis of the amount of charge needed to cause levitation (where the magnitude of the electrostatic force equals or exceeds that of the gravitational force) for several geometries above both Earth and Itokawa, which can be easily extended to other bodies
- Extended bodies can also be treated using the same formalism
- The simulations can readily be expanded to find the equilibrium force as a function of geometry, mass, charge, and levitation height of both the body and the E-Glider

Pre-Decisional Information -- For Planning and Discussion Purposes Only
© 2016 California Institute of Technology. Government sponsorship acknowledged.
marco.b.quadrelli@jpl.nasa.gov

NEO Missions

Station Keeping

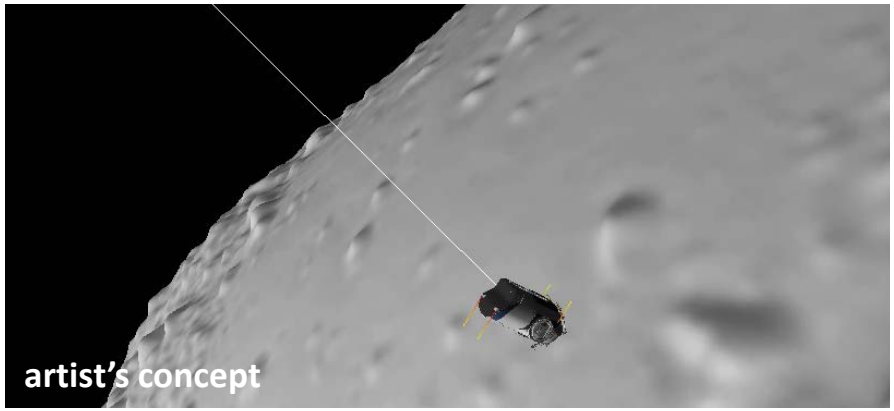

Anchoring

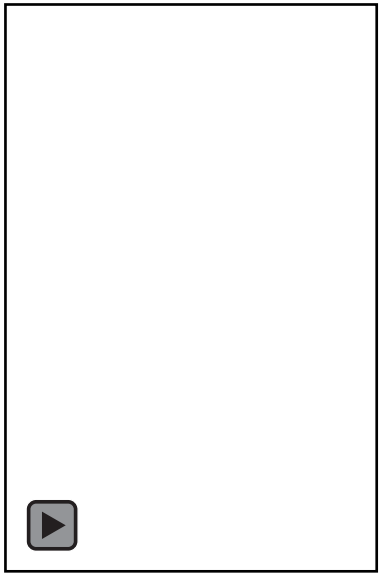

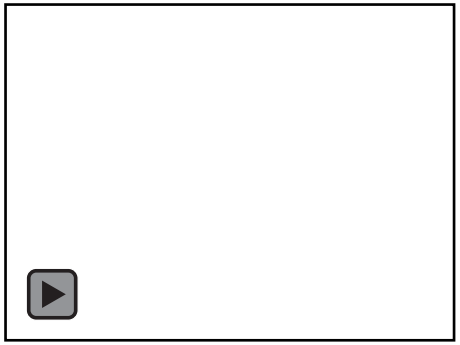

NEO Capture

Anchoring Control

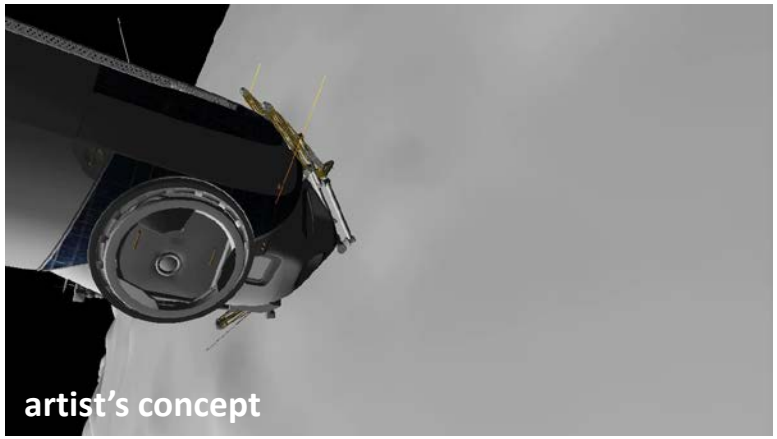

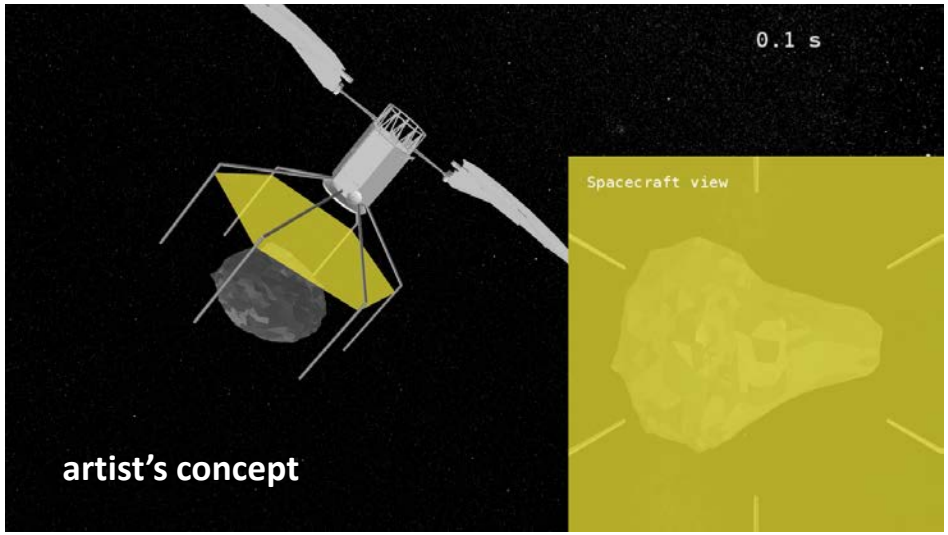

Courtesy of DARTSLab members

Pre-Decisional Information -- For Planning and Discussion Purposes Only
© 2016 California Institute of Technology. Government sponsorship acknowledged.

marco.b.quadrelli@jpl.nasa.gov

DSENDS Simulations

The simulations were started with different initial velocities and positions. The gravity model assumes both bodies are spherical and considers the mass of Itokawa is 3.51 x 10^{10} kg (A. Fujiwara et al Science 2006) and the mass of the E-Glider to be 1 kg.

Pre-Decisional Information -- For Planning and Discussion Purposes Only
© 2016 California Institute of Technology. Government sponsorship acknowledged.

marco.b.quadrelli@jpl.nasa.gov

JPL 150 m Solar Sail Charging Analysis

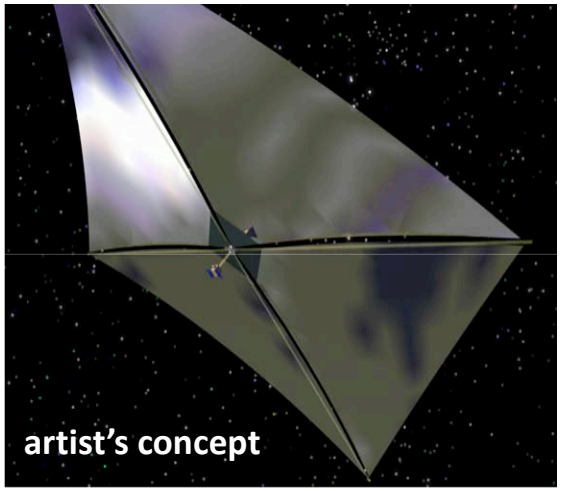

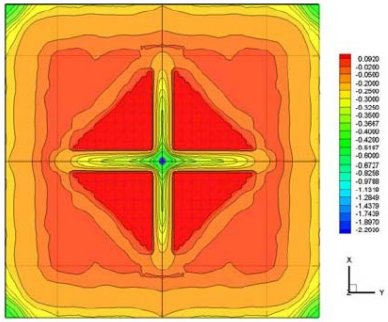

Potential iso-surfaces surrounding the spacecraft (contour levels normalized by Te)

Surface Charging Analysis Findings:

- Nascap predicts differential potentials of many tens of volts across thickness of solar sail membranes with an insulating back in solar wind environments.
- Kilovolt potentials can develop in a geosynchronous substorm environment.
- Greatest potentials developed on the insulating support structures.
- An equipotential spacecraft surface reduces (or eliminates) differential charging minimizing threat of small discharges which could damage the thin film sail.
- Solar sail designs should minimize the use of dielectrics and floating conductors

Solar Sail:
Front – Aluminum
Back - Kapton
Hypotenuse = 150 m
Spacecraft body:
Aluminum
Solar Arrays front
– Solar Cells
Solar Array back
– Black Kapton
Boom connecting Spacecraft and Solar Array craft
- Kapton

Sail simulated as infinitely-thin conducting plate.

1 AU
<u>Environment</u>
N_e = 12.8 cm^{-3}
T_e = 11.13 eV
v_i = 327 km/s
E_i = 558.2 eV
sun in +z direction

Boom: -4 to -53 V
Sail front: 6.5 V
Sail back: -19 V
Spacecraft: 6.5 V
Solar Array:
front: 6.1 to -6.3 V
back: 6.5 V

Differential Φ: ~ 26 V

- 3-D, Electrostatic Particle-in-Cell (PIC) code
- Solar Wind protons treated as particles
- Solar Wind electrons treated as isothermal fluid (Boltzmann distributed)

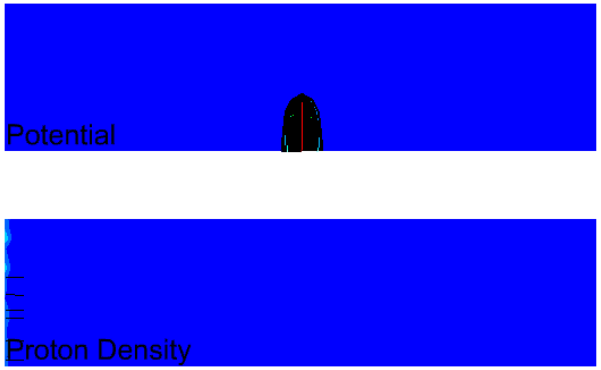

Immersed-Finite-Element PIC (IFE-PIC) algorithm [Lin & Wang, 2003]

Courtesy of Henry Garrett, JPL

© 2016 California Institute of Technology. Government sponsorship acknowledged.
marco.b.quadrelli@jpl.nasa.gov

Charging Environments

	1 AU nominal* Environment 1	1 AU extreme[ξ] Environment 2	½ AU nominal* Environment 1	½ AU extreme[ξ] Environment 2	Geo worst case[ζ]
Electron density	12.8 cm^{-3}	3.28 cm^{-3}	4.27 cm^{-3}	13.1 cm^{-3}	1.12 cm^{-3}
Electron temperature	11.13 eV	55.4 eV	10.6 eV	68.2 eV	12 keV
Ion velocity	327 km/s	863 km/s	702 km/s	863 km/s	
Ion Energy / temp	558.2 eV	3888 eV	2573 eV	3888 eV	29.5 keV
Ion density					0.236 cm^{-3}
Debye length	7 m	31 m	6 m	17 m	770 m
Sun	Intensity = 1, Angle incident: normal, 30° and 55° from sail normal	Intensity = 1, Angle incident: normal, 30° and 55° from sail normal	Intensity = 4, Angle incident: normal, 30° and 55° from sail normal	Intensity = 4, Angle incident: normal, 30° and 55° from sail normal	Intensity = 1, Angle incident: 30° and 55° from sail normal

*Feldman, et al., *Plasma and Magnetic Fields From the Sun,in the Solar Output and Its Variation*, Table 4, 1977.

[ζ] Bame, S.J., D.J. McComas, B.L. Barraclough, J.L. Phillips, K.J. Sofaly, J.C. Chavez, B.E. Goldstein, R.K. Sakurai, The Ulysses Solar Wind Plasma Experiment, Astronomy and Astrophysics, Supplement Series, Ulysses Instruments Special Issue, Vol. 92, 237 – 265, 1992.

[ξ] C. K. Purvis, H. B. Garrett, A. C. Whittlesey, N. J. Stevens, *Design Guidelines for Assessing and Controlling Spacecraft Charging Effects*, NASA TP 2361, 1984.

Courtesy of Henry Garrett, JPL

© 2016 California Institute of Technology. Government sponsorship acknowledged.
marco.b.quadrelli@jpl.nasa.gov

Surface Potential Summary: Solar Wind, 1.0 AU

Environment	Environment #1				Environment #2		
Sail back	Insulating	Insulating	Conducting	Insulating	Insulating	Insulating	Insulating
Angle	Normal	30°	30°	55°	Normal	30°	55°
Exposed Conductor / Sail front	6.684	6.315	5.104	5.349	10.57	9.9	8.13
Sail back	-42.45	-42.46	5.104	-42.48	1.92	1.89	1.72
Solar array	4.648 to 6.538	3.347 to 5.2	5.104 to 6.056	3.223 to 5.148	8.2 to 9.09	8.42 to 9.76	6.72 to 8.24
Boom/sunlight		-77.75	-4.741 to -77.80	-4.019 to -77.77		1.65 to 7.04	3.12 to 8.83
Boom/eclipse	-77.75	-42.46 to -77.75	-19.98 to -77.80	-77.77	1.69	1.65	3.12
Max Differential Potential from Sail front/back	49.13	48.78	0	47.83	8.65	7.98	6.41

Courtesy of Henry Garrett, JPL

Pre-Decisional Information -- For Planning and Discussion Purposes Only
© 2016 California Institute of Technology. Government sponsorship acknowledged.

marco.b.quadrelli@jpl.nasa.gov

Levitation in charged environment

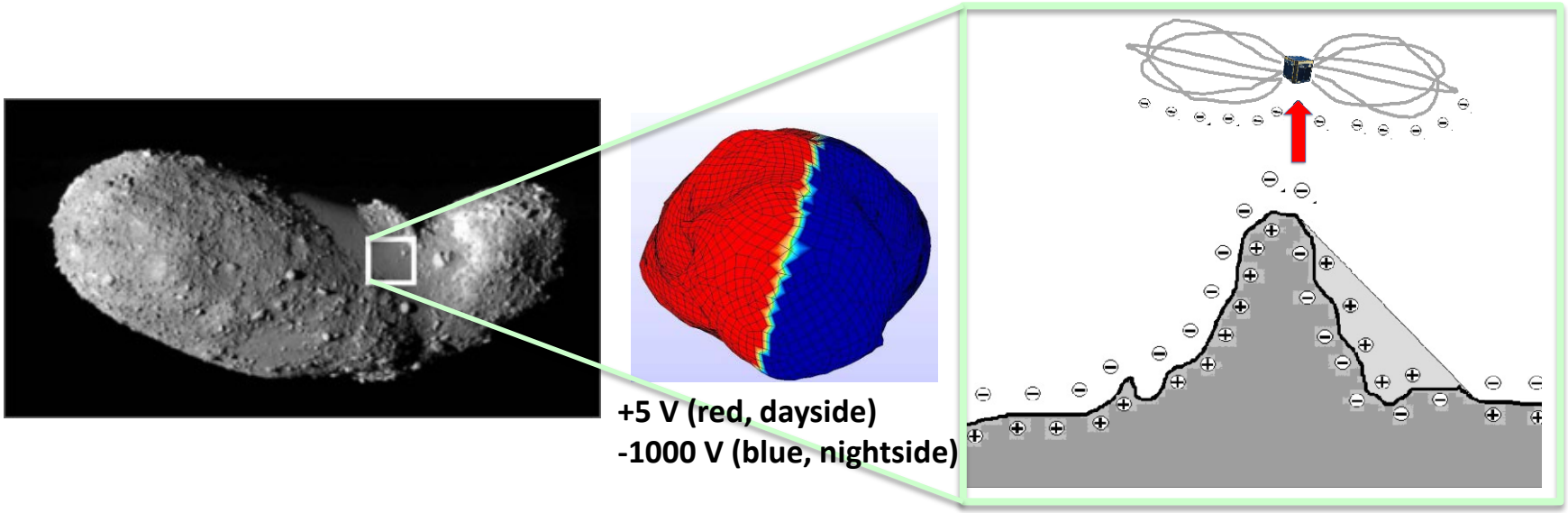

The environment near the surface of airless bodies (asteroids, comets, Moon) is electrically charged due to interactions with the solar wind plasma and UV radiation.

Charged dust is ever present, in the form of dusty plasma [Vladimirov]. Comets have a gas tail and a second electrostatic tail. This environment is also largely unexplored.

Pre-Decisional Information -- For Planning and Discussion Purposes Only
© 2016 California Institute of Technology. Government sponsorship acknowledged.

marco.b.quadrelli@jpl.nasa.gov

Langmuir probe

- Use array of Langmuir probes, which measure the spatial distribution of the charges surrounding the vehicle, to generate an “electrostatic map”.

- One of two Langmuir probes from the Swedish Institute of Space Physics in Uppsala on board ESA's space vehicle Rosetta, due for a comet. The probe is the spherical part, 50 mm in diameter and made from titanium with a surface coating of titanium nitride.

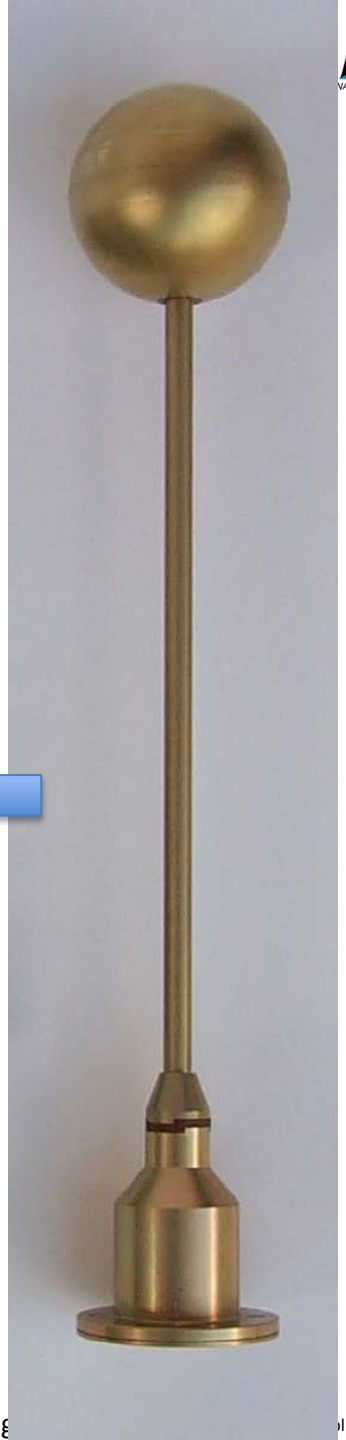

Vehicle with probes

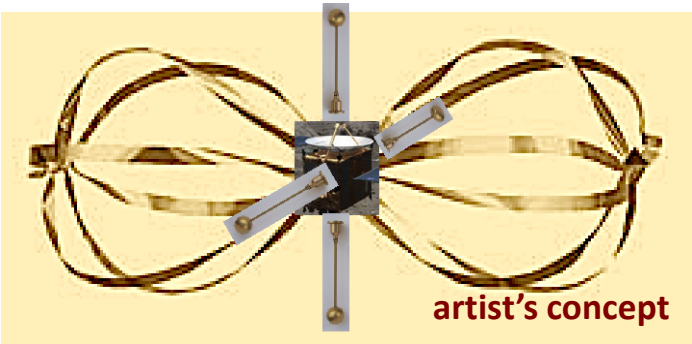

Pre-Decisional Information -- For Planning and Discussion Purposes Only
© 2016 California Institute of Technology. Government sponsorship acknowledg

Autonomous E-glider dynamics & control

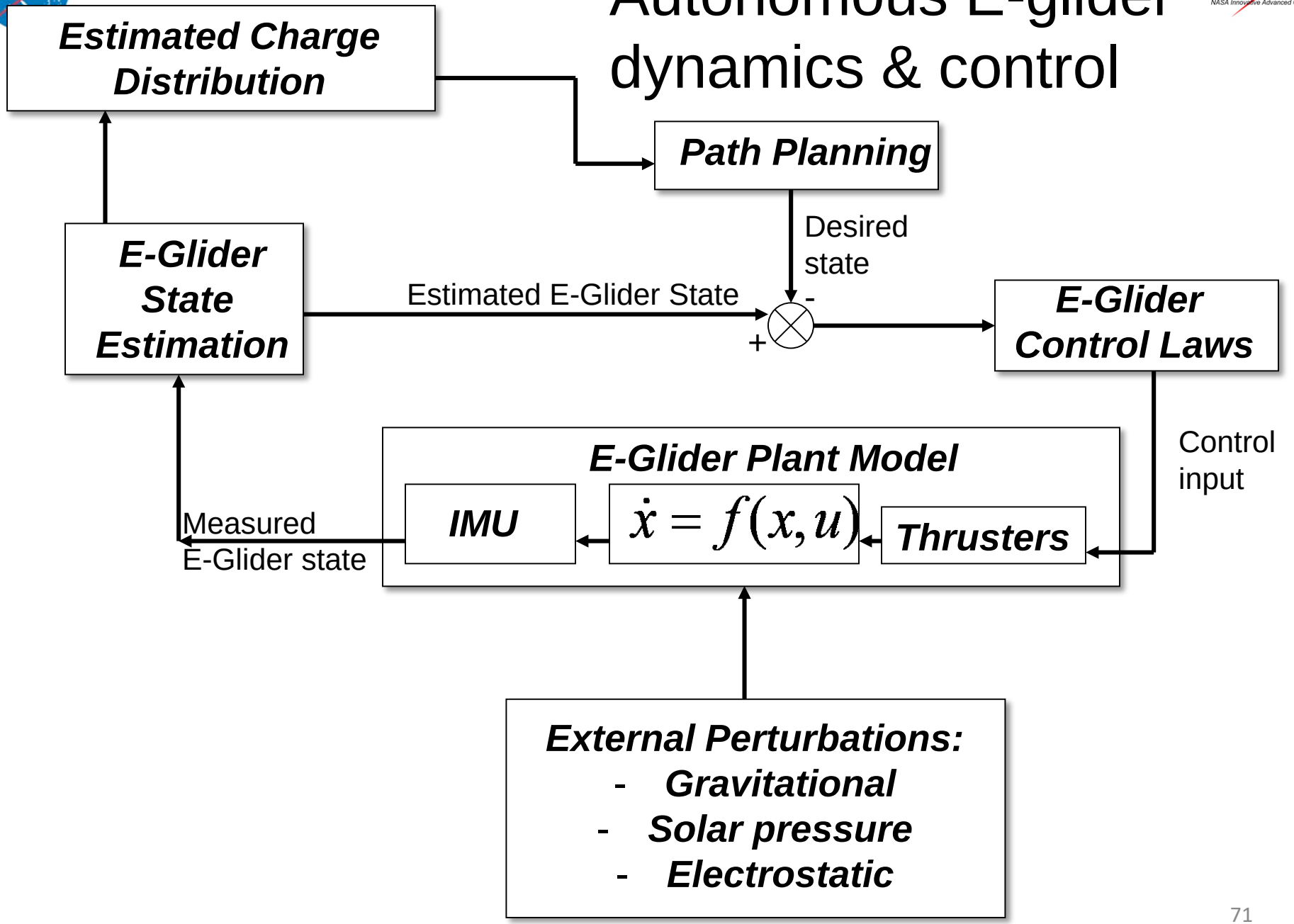

Pre-Decisional Information -- For Planning and Discussion Purposes Only
© 2016 California Institute of Technology. Government sponsorship acknowledged.

marco.b.quadrelli@jpl.nasa.gov

Electro-cartographic navigation

- Once the electric potential has been mapped, the E-glider is able to use this “electrostatic topographic map” for path planning and navigation.

- A potential field approach to path planning for navigation is one path-planning candidate algorithm.

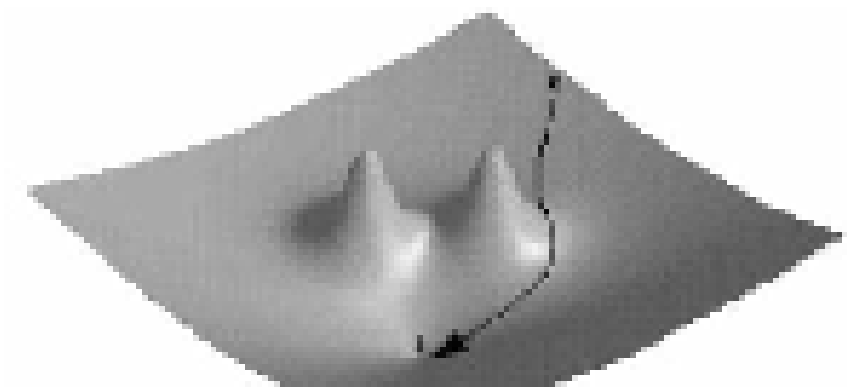

Charge estimation problem

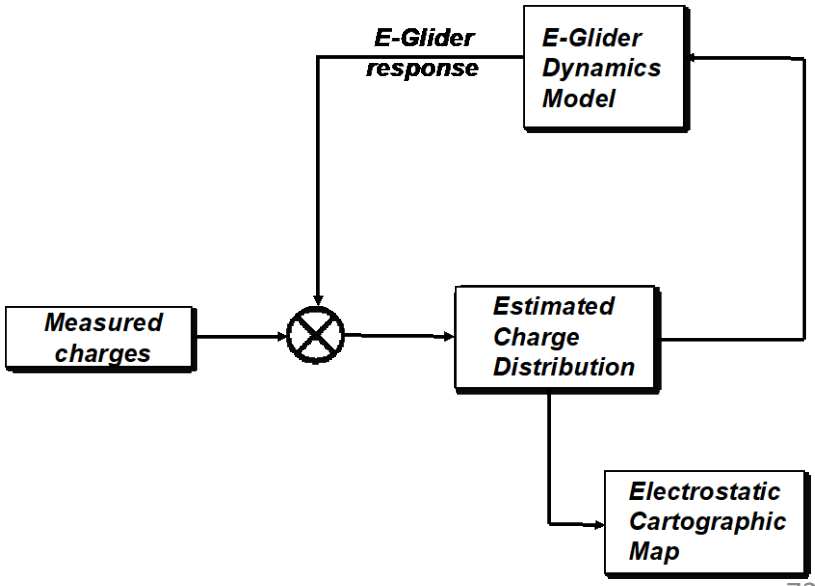

Pre-Decisional Information -- For Planning and Discussion Purposes Only
© 2016 California Institute of Technology. Government sponsorship acknowledged.

marco.b.quadrelli@jpl.nasa.gov

E-Glider risk-based mobility analysis

- JPL's CEMAT = Combined EDL-Mobility Analysis Trade Study Tool
- Optimizes landing ellipse, surface path, and EDL control policy within a given bound on the probability of landing failure

Input

- Terrain (hazard/rock/slope maps)
- Science targets
- Lander/rover design params (control authority, rover size, etc)
- Bound on the probability of landing failure (e.g., 1%)

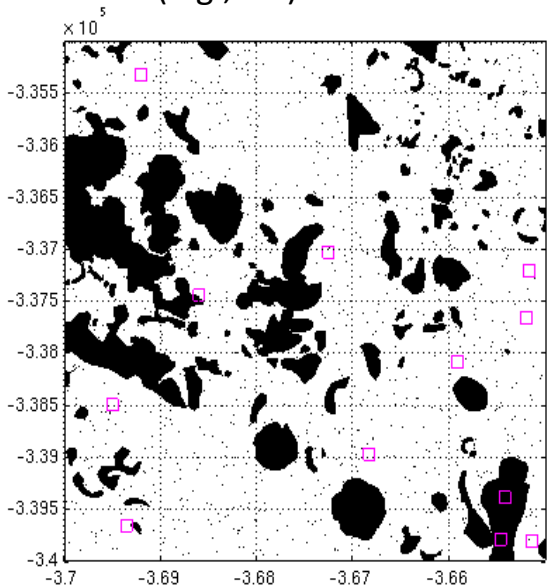

CEMAT

Output

- Expected driving distance to visit a specified number of science target
- Resulting probability of landing failure
- Landing ellipse
- Optimal surface path
- EDL control policy

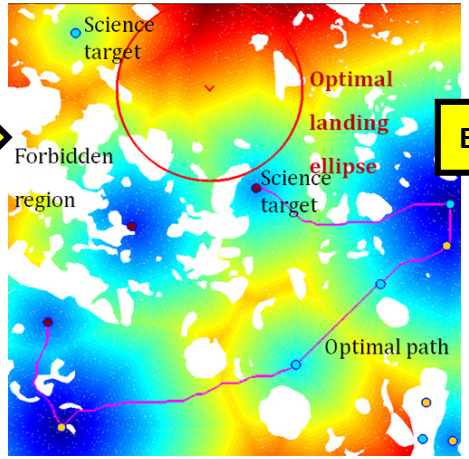

E-CEMAT

Adapt to E-Glider

Given:

- Charge map
- Science targets
- Lander/rover design params (control authority, rover size, etc)
- Bound on the probability of landing failure (e.g., 1%)
- Expected GLIDING distance to visit a specified number of science target
- Resulting probability ure
- 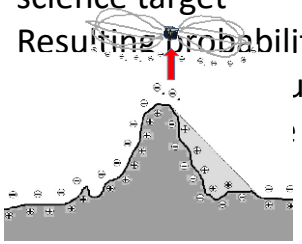
- control policy

Courtesy of Hiro Ono, JPL

Pre-Decisional Information -- For Planning and Discussion Purposes Only
© 2016 California Institute of Technology. Government sponsorship acknowledged.

marco.b.quadrelli@jpl.nasa.gov

E-Glider as mothercraft for large scale science

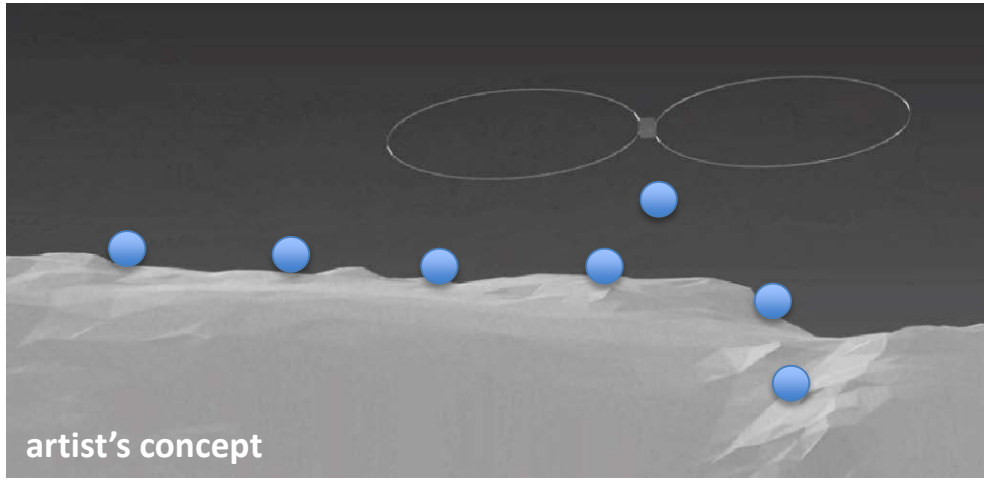

- Deploy electrostatically inflated spherical shells toward surface
- Deform shell surface dielectrically to provide locomotion without gravity

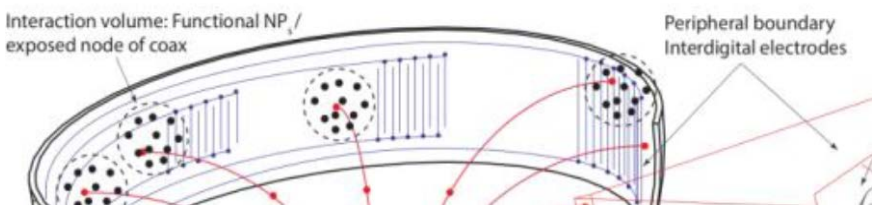

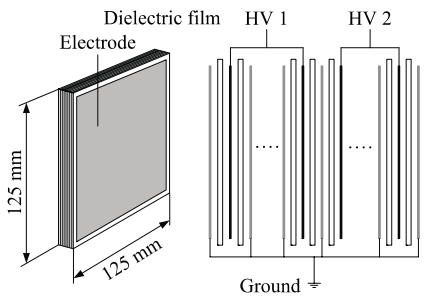

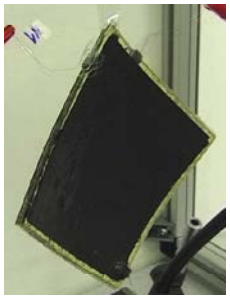

Source: Lochmatter, P., Diss. ETH. No. 17221

Pre-Decisional Information -- For Planning and Discussion Purposes Only
© 2016 California Institute of Technology. Government sponsorship acknowledged.

marco.b.quadrelli@jpl.nasa.gov

Phase I and Phase II Plans

Task	Phase I	Phase II
Concept definition for Small Body application	✓	
Electrostatic dust environment characterization	✓	×
Autonomy/Maneuverability assessment	×	×
Electromechanical actuation assessment	×	
Determination of key miniaturization requirements for science instruments	✓	
System trades	×	×
Preliminary assessment of simulation needs	✓	
Demonstration of flight system performance in simulation		×
PIC plasma simulations in charged environment		×
Proposed experimental efforts	×	
Identify technology gaps for selected architectures, roadmap	×	
E-Glider prototype		×

© 2016 California Institute of Technology. Government sponsorship acknowledged.
marco.b.quadrelli@jpl.nasa.gov

E-GLIDER

THANK YOU!!!

marco.b.quadrelli@jpl.nasa.gov

Pre-Decisional Information -- For Planning and Discussion Purposes Only
© 2016 California Institute of Technology. Government sponsorship acknowledged.